



Spain | 2017

Paolo Borlenghi

Deployment of a low-cost digital platform for the monitoring  
of Santa Maria del Mar church in Barcelona.



ADVANCED MASTERS IN STRUCTURAL ANALYSIS  
OF MONUMENTS AND HISTORICAL CONSTRUCTIONS

# Master's Thesis

Paolo Borlenghi

**Deployment of a low-cost  
digital platform for the  
monitoring of Santa Maria del  
Mar church in Barcelona.**



UNIVERSITAT POLITÈCNICA  
DE CATALUNYA



Education and Culture

**Erasmus Mundus**



ADVANCED MASTERS IN STRUCTURAL ANALYSIS  
OF MONUMENTS AND HISTORICAL CONSTRUCTIONS

# Master's Thesis

Paolo Borlenghi

## **Deployment of a low-cost digital platform for the monitoring of Santa Maria del Mar church in Barcelona.**

This Masters Course has been funded with support from the European Commission. This publication reflects the views only of the author, and the Commission cannot be held responsible for any use which may be made of the information contained therein.



## DECLARATION PAGE

Name: Paolo Borlenghi

Email: paolo.borlenghi@outlook.it

Title of the Msc Dissertation: Deployment of a low-cost digital platform for the monitoring of Santa Maria del Mar church in Barcelona

Supervisors: Rolando Chacón and Luca Pelà

Year: 2017

I hereby declare that all information in this document has been obtained and presented in accordance with academic rules and ethical conduct. I also declare that, as required by these rules and conduct, I had fully cited and referenced all material and results that are not original to this work.

I hereby declare that the MSc Consortium responsible for the Advanced Masters in Structural Analysis of Monuments and Historical Constructions is allowed to store and make available electronically the present MSc Dissertation.

University: Technical University of Catalonia (UPC), Spain

Date: 14/07/2017

Signature: \_\_\_\_\_





## ACKNOWLEDGMENT

I would first like to thank my supervisors prof. Luca Pelà and prof. Rolando Chacón of the School of Civil Engineering at the Technical University of Catalonia. They offered me the possibility to continue this amazing research on low-cost open-source devices that gave me the opportunity to learn so many things in such a short time.

Besides my supervisors, I would also like to thank the expert involved in the development of SmartLab device: Oriol Texidó. Without his patience and fundamental assistance, the Raspberry Pi connection to SmartLab could not have been successfully done.

I would also like to acknowledge Tomás Garcia, the director of the Laboratory of Technology Structures and Materials, and Carlos Hurtado Gómez for the great help with sensors and calibration tests.

I would like to acknowledge the engineer Camilo Basto for his enthusiasm and dedication to this topic.

Furthermore, I would like to express my gratitude to the SAHC Consortium and the Erasmus Mundus Programme that offered me the opportunity to participate with the financial support of a scholarship.

Finally, I would like to thank the Parish of Santa Maria del Mar and the architects Jordi Ninot Pie and Jordi Portal Liaño for the unique opportunity to work in this beautiful place.

This research has received the financial support from the MINECO (Ministerio de Economía y Competitividad of the Spanish Government) and the European Regional Development Fund (ERDF) through the MULTIMAS project (Multiscale techniques for the experimental and numerical analysis of the reliability of masonry structures, ref. num. BIA2015-63882-P).

*The miracle is this - the more we share, the more we have.*

*(Leonard Nimoy)*

## ABSTRACT

Despite the growing need of protection for Cultural Heritage, many technological innovations are held back by the lack of affordable hardware. In this sense, Structural Health Monitoring (SHM) is a highly valuable tool for the vulnerability assessment of historical constructions, but its wide diffusion is limited by the high costs, both implementation and operation. For this reason, there is currently the need for SHM strategies with cost reduction but still able to ensure good performance.

The objective of the study is to contribute to the development of a low-cost, open-source, reliable and accurate system for the structural monitoring of architectural heritage. The first phase of the research includes the selection of open-source hardware and low-cost strategies based on past projects at the Department of Civil and Environmental Engineering of Polytechnic University of Catalonia- Barcelona Tech and market analysis. The second phase focuses on the system calibration and evaluation of experimental resolution and accuracy, including extensive analysis of analog-to-digital converter (ADC) and linear potentiometer reliability. The third phase describes the deployment of the system in Santa Maria del Mar church in Barcelona. The results of the research show the great potential of this technology that may help to promote a comprehensive and cost-efficient monitoring of the built cultural heritage.

Keywords: Arduino, Raspberry Pi, Open-source hardware, Structural Health Monitoring; Continuous Monitoring, Cultural Heritage.



## RESUMEN

A pesar de la creciente necesidad de proteger el Patrimonio Cultural, muchas investigaciones tecnológicas se mantienen paralizadas por falta de equipos y herramientas asequibles que motiven su desarrollo. En este sentido, *Structural Health Monitoring* (SHM) se considera una valiosa herramienta para la evaluación de la vulnerabilidad de las construcciones histórica, no obstante, su alcance está limitado por los altos costes de implementación y operación. Por esta razón, hoy en día existe la necesidad de llevar a cabo estrategias de SHM de bajo coste y capaces de garantizar un buen rendimiento.

El objetivo de este estudio es contribuir al desarrollo de un sistema de monitoreo estructural para el patrimonio arquitectónico con características *low-cost*, de código abierto y que además arroje resultados fiables y de precisión. La primera fase de esta investigación incluye la selección del equipo de código abierto y las estrategias para reducir los costes de implementación basándose en investigaciones anteriores desarrolladas en el Departamento de Ingeniería Civil y Ambiental de la Universidad Politécnica de Cataluña – Barcelona Tech y estudios de mercado. La segunda fase se enfoca en la calibración del sistema y la evaluación experimental de la resolución y la precisión del mismo, incluyendo Conversor Analógico Digital (ADC) y eficacia del potenciómetro lineal. La tercera parte desarrolla el despliegue del sistema en la Basílica de Santa María del Mar (Barcelona). Los resultados de la investigación muestran el gran potencial de esta tecnología que puede ser útil para promover un monitoreo integral y rentable del patrimonio construido.

Palabras claves: Arduino, Raspberry Pi, Open-source hardware, Structural Health Monitoring; Continuous Monitoring, Patrimonio Cultural.



## Table of Contents

1	Introduction.....	1
1.1	Motivation of the research.....	1
1.2	Main aim and specific objectives.....	2
1.3	Outline of the thesis.....	4
2	State-of-the-Art .....	5
2.1	Review of Structural health monitoring standards.....	5
2.1.1	SHM components.....	6
2.1.2	SHM categories .....	7
2.1.3	Advantages and Limitations.....	8
2.2	Review of displacement control systems.....	9
2.2.1	Linear Variable Differential Transformer .....	9
2.2.2	Linear Potentiometer.....	10
2.3	Review of open source and digital fabrication technologies .....	11
2.3.1	Open-source technologies for Science.....	13
2.4	Reviews of Microcontroller boards and Single-board computers.....	13
2.4.1	Arduino board .....	13
2.4.2	Internet of Things and Raspberry Pi.....	14
2.5	Review of low-cost sensors for structural monitoring.....	15
2.5.1	Texas Instruments' LM35 temperature device.....	15
2.5.2	Adafruit's DHT11 and DHT22 temperature and humidity sensors.....	16
2.5.3	Displacement control devices .....	17
2.6	Final remarks .....	18
3	Previous experiences in structural low-cost monitoring .....	19



3.1	First experience at UPC by Basto (2015).....	19
3.1.1	Results obtained .....	21
3.1.2	Comments .....	23
3.2	Second experience at UPC by Martinez (2017) .....	23
3.2.1	Stakeholder involvement.....	23
3.2.2	System proposed by Martinez.....	24
3.2.3	Results obtained .....	26
3.2.4	Comments .....	27
3.3	Lessons learned from previous experiences at UPC.....	28
3.3.1	Energy supply .....	28
3.3.2	Measures and sensors .....	28
3.3.3	Data acquisition system (DAS).....	28
3.3.4	Data transmission system (DTS) .....	29
4	Implementation of a new low-cost structural monitoring system .....	31
4.1	Useful concepts of metrology, electronics and signal processing .....	31
4.1.1	Accuracy, Precision, Sensitivity and Resolution .....	31
4.1.2	Analog-to-Digital converter (ADC).....	33
4.1.3	Overview of noise analysis in electronic circuits .....	34
4.2	Components selection .....	35
4.2.1	DAS selection .....	35
4.2.2	Sensors selection: displacement .....	38
4.2.3	Sensors selection: temperature and humidity.....	40
4.2.4	Data transmission system (DTS) and energy supply .....	43
4.2.5	Final remarks.....	43

4.3	Laboratory test: linear potentiometer.....	45
4.3.1	System set-up .....	46
4.3.2	Noise filtering .....	51
4.3.3	Calibration of the Novotechnik TEX 0050 .....	54
4.3.4	Final remarks .....	59
4.4	Further improvements: strategies for building a reliable system.....	62
4.4.1	Introduction: a new block diagram for the linear potentiometer .....	62
4.4.2	Precision voltage reference.....	63
4.4.3	The Novotechnik linear potentiometer.....	63
4.4.4	External ADC.....	64
4.4.5	Final remarks .....	64
5	Deployment on a Cultural Heritage building: Santa Maria del Mar .....	65
5.1	Introduction on the problem .....	65
5.2	Historical information.....	66
5.3	General description of the building.....	67
5.4	Monitoring proposals.....	68
5.5	Design of the system set-up .....	69
6	Conclusions.....	73
6.1	Summary.....	73
6.2	Specific conclusions .....	74
6.3	General observations .....	75
6.4	Suggestion for future improvements.....	76
7	Bibliography.....	79



## List of Figures

Figure 1: Dynamic monitoring system of the San Vittore's bell-tower in Arcisate, Italy (Gentile et al., 2012) .....	5
Figure 2: Components of a typical SHM system (Bisby and ISIS Education Committee, 2005) (left), a static monitoring system with a traditional displacement transducer and optical camera on "Sala dei Battuti" of Conegliano, Italy (Lorenzoni et al., 2015) (right). .....	6
Figure 3: Categories of SHM system (Bisby and ISIS Education Committee, 2005).....	7
Figure 4: General strategies for the study and evaluation of architectural heritage Niker project, WP9) .....	8
Figure 5: Schematic of Linear Variable Differential Transformer (LVDT) (Dunnicliff, 1993) .....	9
Figure 6: Schematic of Linear Potentiometer (Dunnicliff, 1993) .....	10
Figure 7: The rise of open software and the promising era of open hardware (Rambus website)	11
Figure 8: Cosmic Pi: Raspberry Pi-based cosmic ray detector (left-up); Parametric cuvette and vial rack (right-up); OpenPCR: DNA analysis (left-down); RepRap: self-replicating rapid prototype (right-down) .....	12
Figure 9: Arduino UNO (left) and Arduino MEGA (right).....	14
Figure 10: LM35 pin configuration (left) and diagram of maximum temperature error over operating temperature (right) .....	15
Figure 11: DHT11 pin configuration (left) and DHT22 pin configuration (right) .....	16
Figure 12: Tell-tale crack meter with a digital calliper.....	17
Figure 13: Low-cost structural monitoring elements' diagram (Basto, 2015).....	19
Figure 14: Basto's Temperature system (Basto, 2015) .....	20
Figure 15: System workflow according to Basto.....	21
Figure 16: A solder-less breadboard .....	21
Figure 17: Internal temperature and humidity, and external temperature distribution over time (Basto, 2015).....	22
Figure 18: Displacement evolution and internal temperature distribution over time (Basto, 2015) .....	22
Figure 19: System developed by Martinez for the deployment of low-cost structural monitoring in Santa Maria del Mar (Martínez Gil, 2017).....	25

Figure 20: The logo of SmartLab device.....	25
Figure 21: System installed by Martinez in the block B1 of the UPS's Northern campus (Martínez Gil, 2017) .....	26
Figure 22: Temperature and displacement recorded between 25 January 2017 and 29 January 2017 by Martinez (Martínez Gil, 2017) .....	27
Figure 23: Temperature and displacement recorded between 11 April 2017 and 15 April 2017 by Martinez (Martínez Gil, 2017) .....	27
Figure 24: Implementation of a new low-cost structural monitoring system .....	31
Figure 25: Difference in Accuracy and Precision .....	32
Figure 26: Analog-to-Digital converts: 12-bit Adafruit's ADS1015 (left); 10-bit Maxim Integrated's MAX177 (center); 16-bit Texas Instruments' DAC8830 (right).....	33
Figure 27: Significant bits (Mancini, 2002) .....	34
Figure 28: Voltage noise signal in the time domain (T. C. Carusone, D. A. Johns, 2012) .....	35
Figure 29: Linear potentiometer's data correspondence with Arduino DUE.....	40
Figure 30: Temperature sensors test .....	41
Figure 31: Humidity sensors test.....	41
Figure 32: DHT22 cable length sensitivity .....	42
Figure 33: System set-up for Santa Maria del Mar .....	44
Figure 34: System set-up for laboratory testing .....	45
Figure 35: Potentiometer installed on the Displacement Transducer Calibration Device (resolution 0.002 mm).....	46
Figure 36: 1053 samples of Novotechnik TEX 0050's noise in a stationary position.....	47
Figure 37: Gaussian distribution of 1053 samples.....	47
Figure 38: 2350 samples of Novotechnik TEX 0050's noise in a stationary position.....	48
Figure 39: Gaussian distribution of 2350 samples.....	49
Figure 40: 520 samples of Novotechnik TEX 0050's noise in a stationary position.....	49
Figure 41: Gaussian distribution of 520 samples.....	50
Figure 42: Standard deviation over number of samples of 2350 samples.....	51
Figure 43: Averaging of the 2350 sample records with an interval on 16 samples .....	52
Figure 44: Averaging of the 2350 sample records with an interval on 50 samples .....	52

Figure 45: Running average of the 2350 sample records with an array of 50 elements.....	53
Figure 46: Running average of the 2350 sample records with an array of 500 elements.....	54
Figure 47: Data acquisition and data processing workflow at Camins Maker Lab 16/07/2017 ...	55
Figure 48: Complete recordings of calibration experiment at Camins Maker Lab 16/07/2017 ...	55
Figure 49: Voltage spikes on collected data .....	56
Figure 50: Filtered data without significant fluctuation (StdDev=2,74).....	60
Figure 51: Filtered data with significant fluctuation (StdDev=3,85) .....	60
Figure 52: Filtered data with a significant increase of noise (StdDev=4,36) .....	61
Figure 53: Typical Block Diagram of a Transducer Measurement System .....	62
Figure 54: Shown configuration for extended position of the actuating rod (left) and schematic view of wiring (right): 1 power, 4 signal and 3 ground .....	64
Figure 55: Santa Maria del Mar: interior (left) nave and main façade (right).....	65
Figure 56: Plan of the church and the position of the two cracks .....	66
Figure 57: Before (left) and after (right) the fire of 1936 (Martínez Gil, 2017) .....	67
Figure 58: Monitoring proposal .....	70

## List of Tables

Table 1: Systems built for the monitoring campaign (Basto, 2015).....	20
Table 2: Systems developed by Martinez for the deployment of low-cost structural monitoring in Santa Maria del Mar (Martínez Gil, 2017).....	24
Table 3: Microcontrollers comparison.....	36
Table 4: Displacement's sensors comparison .....	39
Table 5: Temperature's sensors comparison .....	42
Table 6: Standard deviation distribution regarding the number of samples .....	50
Table 7: Calibration of the Novotechnik TEX 0050 .....	58
Table 8: Variation in standard deviation between the 29/05 and the 16/06 .....	59





## 1 INTRODUCTION

### 1.1 Motivation of the research

In the last decades, the need for protection of cultural heritage, has been widely discussed. Particularly, some tragic events highlight the vulnerability of the architectural heritage of Europe: the sudden collapse of the Civic Tower in Pavia, Italy (Binda et al., 2003), the bell-tower of St. Magdalena in Goch, Germany and the cathedral of Noto, Italy (Binda and Saisi, 2003). In this context, Structural health monitoring (SHM) has become a valuable tool that can enhance and increase the structure understanding, reduce uncertainties, and provide accurate data for analysis and intervention. SHM has been already successfully deployed in strategic structures, like bridges, or highly valuable cultural heritage buildings as churches. One of the main barriers to the large-scale diffusion of this technique remains the high costs, both implementation and operation. For this reason, there is currently the need for SHM strategies with reduced costs but still able to ensure good performance.

On the one hand, the open-source community is rapidly growing in popularity between entrepreneurs, designers, computer scientists and hobbyists. Nowadays the market offers a broad assortment of microcontrollers (Arduino<sup>1</sup>, Raspberry Pi<sup>2</sup>, BeagleBoard<sup>3</sup> and Adafruit<sup>4</sup>) with a much lower price compared to professional solutions. Recent research experiences have shown the vast possibilities of open-source hardware and software used in environmental (Ali et al., 2016), structural static (Basto et al., 2017), and structural dynamic monitoring (Chacón and Oller, 2017). This technology is really promising for large-scale application of SHM systems, otherwise too expensive for the majority of historical constructions.

On the other hand, the lack of precision and accuracy is the main weakness of this technology. Especially in the complex context of cultural heritage buildings, there are still no mid- and long-

---

<sup>1</sup> <https://www.arduino.cc/>.

<sup>2</sup> <https://www.raspberrypi.org/>.

<sup>3</sup> <http://beagleboard.org/>.

<sup>4</sup> <https://www.adafruit.com/>.

term applications. Furthermore, the vast majority of SHM sensors (i.e. accelerometers or LVDT) is not easily replaceable with a low-cost version due to reliability and accuracy issues. Conversely, particularly promising are the innovations on acquisition and transmission of data with wireless technologies (Ferdoush and Li, 2014), much cheaper than their professional counterpart.

This research started with the purpose to bring SHM to a site that cannot afford high investments, or simply with the idea to create a more efficient open-source system around a community of researchers and enthusiasts. The diffusion of this methodology could bring to a radical change in the conservation culture, giving the possibility to apply SHM in the daily practice both for university and for professionals. Furthermore, the spread of open-source data on historical structures could considerably increase the knowledge on our built heritage since SHM could be implemented on a bigger number of case studies.

## 1.2 Main aim and specific objectives

The main aim of the present work is to contribute in the development of a low-cost, open-source, reliable and accurate system for the structural monitoring of monumental structures and more broadly of Cultural Heritage (CH). At the current state, some promising results are available but before a long-term deployment a preliminary calibration is needed.

In order to accomplish the main aim of the current research, it was necessary to divide the study in specific objectives:

- (i) Understand the basic principles of Structural Health Monitoring (SHM), including:
  - a. Analysis of the main components and strategies of SHM;
  - b. Focus on the electro-mechanical features of common displacement sensors.
- (ii) Analyse the new market trends in term of low-cost solutions on microcontrollers and sensors, including:
  - a. Open source microcontrollers and microcomputers;
  - b. Instruments for sensing temperature, humidity and displacement.
- (iii) Learn from promising past experience in low-cost structural monitoring, including:

- a. Analysis of the hardware and the software structure, the component used and the results obtained;
  - b. Identification of the main limitations and research the causes.
- (iv) Set up of an improved system to overcome past drawbacks, including the selection of components based cost/performance ratio.
- (v) Perform a preliminary calibration in the laboratory, including:
  - a. Noise and nonlinear ADC effects on the signal;
  - b. Statistical noise filtering techniques;
  - c. Determination of the experimental resolution and the accuracy of the system.
- (vi) Overcome the limitation encountered in the lab testing.
- (vii) Design the continuous static monitoring system for Santa Maria del Mar.

### 1.3 Outline of the thesis

The thesis is organised into seven chapters, according to the path presented in the previous paragraph.

Chapter 1 presents an introduction to the dissertation, focusing on motivations, aims and specific objectives.

Chapter 2 provides a review of Structural Health Monitoring (SHM) applied to civil engineering structures and analyses the world of open-source and digital fabrication technologies. Particular attention is given to sensors for crack monitoring and to the increasing availability of microcontroller boards and single-board computers.

Chapter 3 focuses on previous research experiences in structural low-cost monitoring.

Chapter 4 reports the results of the system calibration and calculation of experimental resolution and accuracy, including extensive analysis of analog-to-digital converter (ADC) and linear potentiometer reliability.

Chapter 5 describes the design of the low-cost monitoring system for Santa Maria del Mar church in Barcelona.

Chapter 6 presents the main conclusions from each chapter and a proposal for future works.

## 2 STATE-OF-THE-ART

The main goal of this chapter is reviewing the available procedures and the most recent stage in the development of the two fields of this thesis: Structural Health Monitoring (SHM) and open-source low-cost digital technologies. SHM is analysed from two points of view: the components and the categories. Particular attention is given to displacement sensor technology since its intrinsic complexity. Furthermore, the philosophy and new trends in open-source technologies are described with a particular focus on low-cost microcontrollers and sensors.

### 2.1 Review of Structural health monitoring standards

The classical vulnerability assessment for cultural heritage is composed of the following steps: historical analysis, geometric survey, decay and deformation mapping, non-destructive (ND) or minor-destructive (MD) tests, laboratory tests on cores and, finally, a numerical or analytical model (Binda et al., 2000). The vast majority of experimental tests barely gives information on the evolution of a certain phenomenon or helps to understand the global behaviour of the structure. To overcome these limitations, a monitoring system is needed.

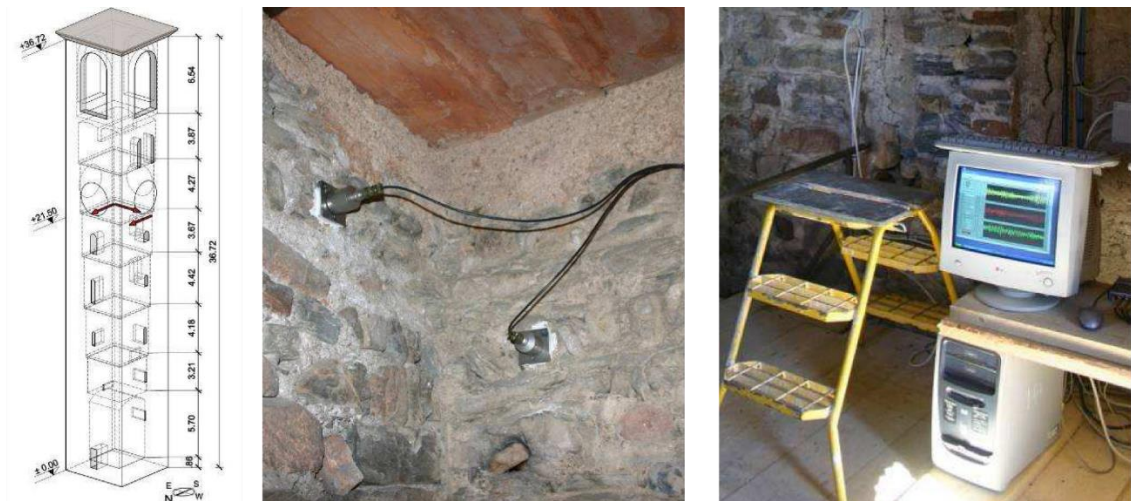


*Figure 1: Dynamic monitoring system of the San Vittore's bell-tower in Arcisate, Italy (Gentile et al., 2012)*

SHM is a set of strategies able to provide real-time continuous data on the health of the structure (Gentile and Saisi, 2007). It is a very powerful tool able to (i) identify, localise and quantify damage, (ii) determine the active physical phenomena involved in the damage process, (iii) provide data for

estimation of safety and remaining life of a building, and (iv) give information on the real structural behaviour before and after the strengthening intervention (Lorenzoni, 2013). Indeed, monitoring can be an alternative to strengthening intervention or minimise the need for it (Ramos et al., 2010).

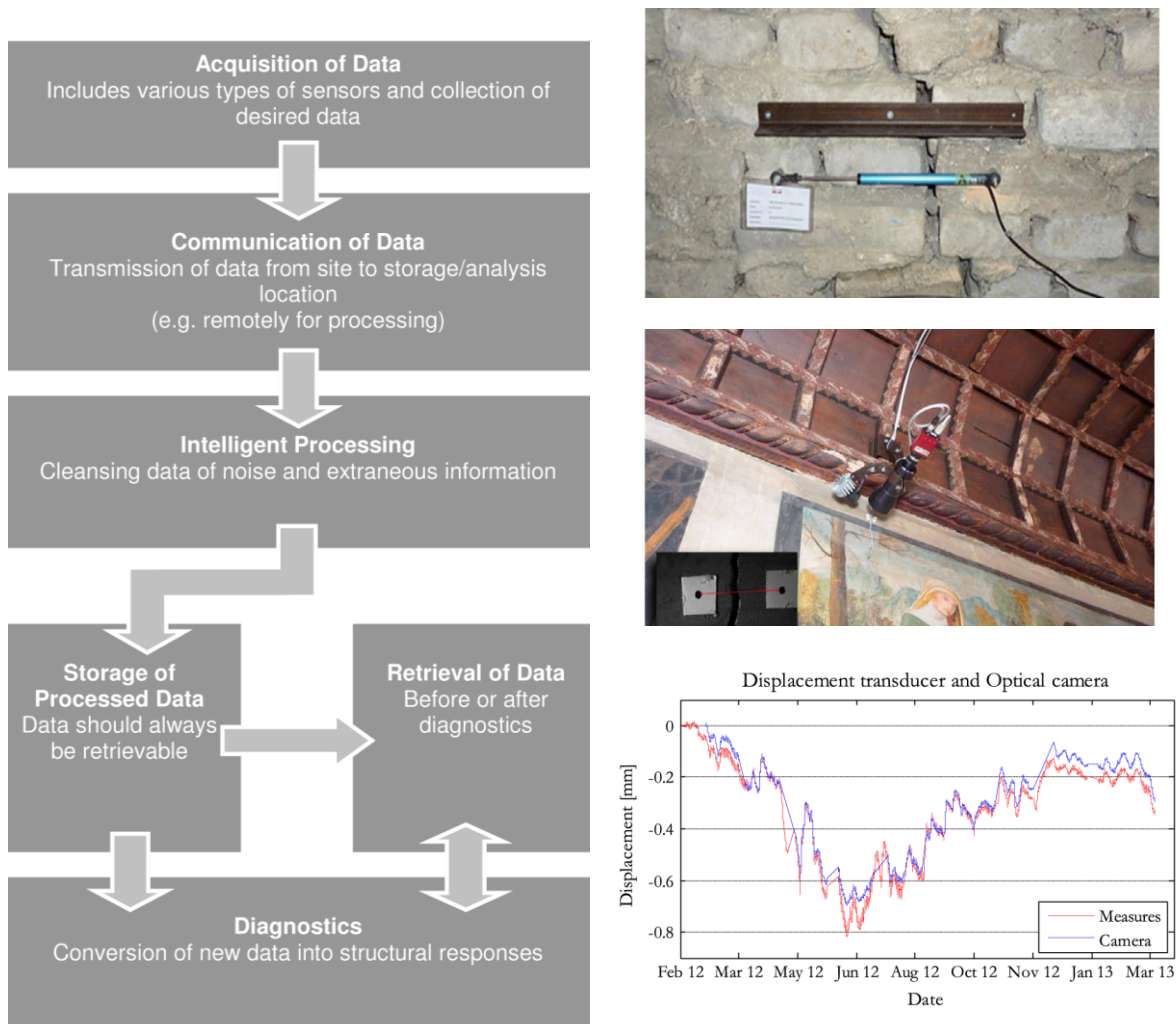


Figure 2: Components of a typical SHM system (Bisby and ISIS Education Committee, 2005) (left), a static monitoring system with a traditional displacement transducer and optical camera on "Sala dei Battuti" of Conegliano, Italy (Lorenzoni et al., 2015) (right).

### 2.1.1 SHM components

As stated by SAMCO (Structural Assessment, Monitoring and Control) association (Bisby and ISIS Education Committee, 2005), an SHM system is composed of six common components: (i) acquisition data (i.e. sensors and data acquisition systems), (ii) communication of information, (iii) intelligent process and analysis of data, (iv) storage of processed data, (v) diagnostics (i.e. damage

detection and modelling algorithms), and (vi) retrieval of information as required. Fig. 2 (left) shown a typical flow pattern for SHM. In the following research, only the first two phases are considered.

*Acquisition and collection of data* involve the collection of raw data such as displacement or strain and environmental parameters as temperature and humidity through a network of sensors. The storage of data, the signal demodulation and conditioning are accomplished by the data acquisition system (DAS). Finally, the *communication of data* is the component that refers to the procedures and systems able to send data from the site to a remote computer where the analysis and post-processing of data are completed.

### 2.1.2 SHM categories

According to SAMCO association (Bisby and ISIS Education Committee, 2005), SHM can be divided into four categories: by the response typology (i) static or (ii) dynamic, or by timescale in (iii) triggered-based, (iv) periodic or continuous monitoring.

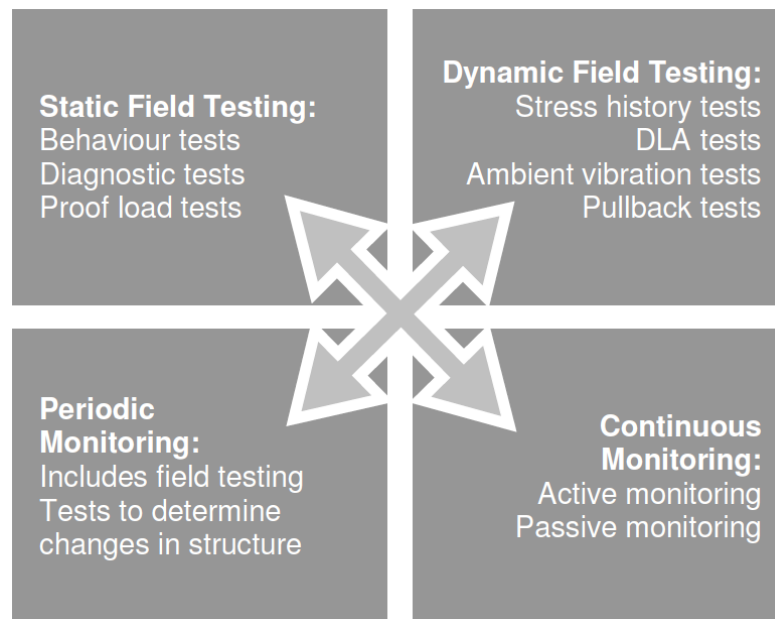


Figure 3: Categories of SHM system (Bisby and ISIS Education Committee, 2005)

*Static-based techniques* are the most common method used to evaluate the actual load carrying capacity of a structure (Bisby and ISIS Education Committee, 2005). They focus on measuring slow changes in the response of the structure: geometrical changes (e.g. displacement and tilt), damage identification (e.g. crack size and pattern), stress and strain or environmental parameters

(e.g. wind speed, humidity or temperature) (Lorenzoni, 2013). The excitation can be known as a slowly applied load, unknown as environmental effects or caused by an active phenomenon (e.g. soil settlements) (Grosso et al., 2004). Crack growth is usually monitored on a *continuous* based. *Dynamic-based techniques* focus on the identification of modal parameters, damages or vibrations from the earthquake, traffic or another live load (Lorenzoni, 2013). It is usually employed as a permanent system capable of capturing the motion of a structure only when a certain threshold occurs (*triggered-based monitoring*). Alternatively, it can control vibration on a periodic basis.

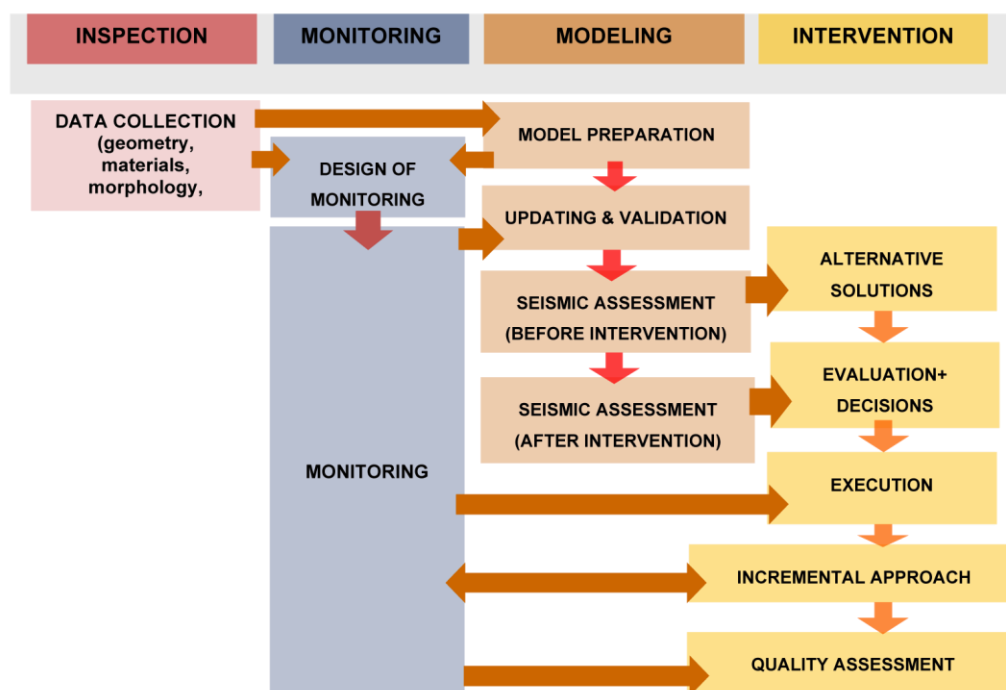


Figure 4: General strategies for the study and evaluation of architectural heritage Niker project, WP9)

### 2.1.3 Advantages and Limitations

As it is clear, the advantages of using SHM are numerous. Structural systems of all kinds can be monitored and decisions can be taken based upon real observations (Figure 4). On the other hand, the main limitation of this technique are the high costs, both implementation and operation. Despite advances in monitoring technology, its wide application is held back due to the lack of affordable hardware. This scarcity of cheap solution is particularly problematic for private citizens or small administration that don't have the same economic resources as well-funded institutions.



## 2.2 Review of displacement control systems

Most displacement monitoring systems consist of a data acquisition system (DAS), a transducer, and the communication system between these two components (Park et al., 2003). A transducer is a device that translates a physical phenomenon into an output signal while the DAS converts the signal into information useful for the interpretation of the physical phenomenon. Generally, the position is measured with mechanical (e.g. micrometres), hydraulic, pneumatic, or electrical transducers. In long-term structural monitoring application, mostly electrical transducers (i.e. Linear Variable Differential Transformer or linear potentiometer) are used (Drdáky, 2005).

### 2.2.1 Linear Variable Differential Transformer

A Linear Variable Differential Transformer (LVDT) is composed of a movable magnetic core passing through one primary coil and two secondary coils. An AC voltage, called excitation voltage, feeds the primary coil, in this manner an AC voltage is introduced in the secondary coil, with a magnitude that depends on the proximity between the magnetic core and the secondary coils. The secondary voltages are connected in series opposition so that the net output of the LVDT is the difference between these two voltages. When the core is at its mid position, the net output voltage is zero. When the core moves off the centre, the net output voltage increases linearly in magnitude with polarity depending on the direction of the core displacement (Dunnicliff, 1993).

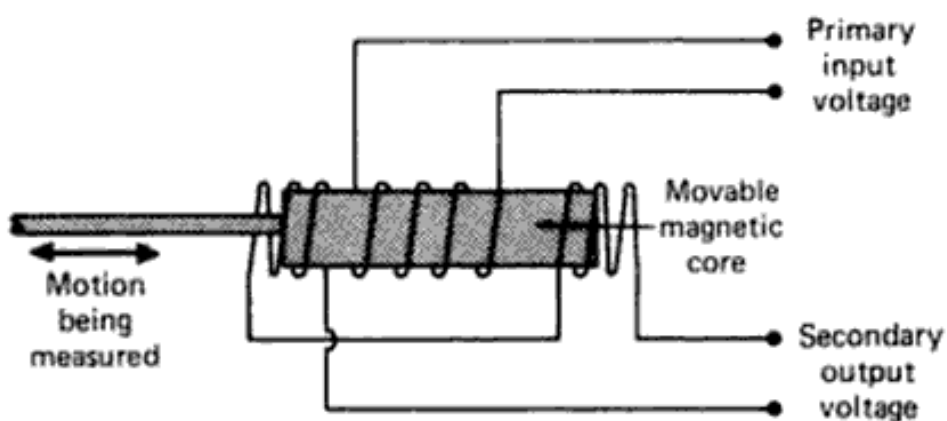


Figure 5: Schematic of Linear Variable Differential Transformer (LVDT) (Dunnicliff, 1993)

The data acquisition system for an LVDT includes a means for generating the excitation voltage, a demodulator/amplifier, and a connection to the transmission system.

Since the core of an LVDT does not contact the coils, friction is avoided. There is no hysteresis and LVDTs are especially suitable for measuring dynamic motions and very small displacements. Many types of LVDT have excellent good long-term stability, and they can be protected within the oil-filled housing to maximise longevity. However, the transmission of alternating current through long lead wires introduces unwanted cable effects, which can seriously degrade the output signal (Dunnicliff, 1993).

### 2.2.2 Linear Potentiometer

Linear potentiometers are an alternative to LVDTs for remote measurement of deformations. A potentiometer (pot) is a device with movable slide, usually called a wiper. That makes electrical contact with a fixed resistance strip. As shown in the figure below, a regulated DC voltage is applied to the two ends of the resistance strip, and the voltage between B and C is measured as the output signal. The voltage varies between the voltage at A and the voltage at B as the wiper moves from A to B (Dunnicliff, 1993).

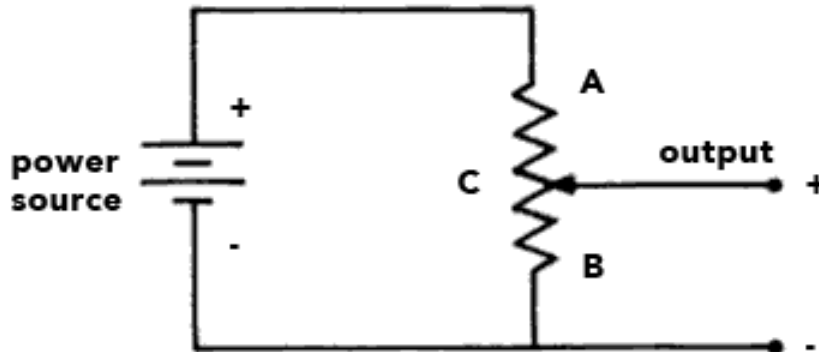


Figure 6: Schematic of Linear Potentiometer (Dunnicliff, 1993)

Potentiometers are not suitable for measuring rapidly varying motions. However, the readout is simple and can be arranged to give a high output voltage, which is not readily degraded by long lead wire effects or electrical noise. Furthermore, potentiometers can successfully be used for long-term monitoring (Dunnicliff, 1993).

### 2.3 Review of open source and digital fabrication technologies

The term “open source” was adopted between 1997 and 1998 to define a software that anyone is freely licensed to use, copy, study or modify (Bretthauer, 2001). Typically, the computer software is distributed as a finished product where the end users are not allowed to see or edit the code. In this case, the company’s developers are the only in charge for bug fixing and customer support, causing a complete dependency from the organisation’s policies (e.g. in the case of development interruption). By contrast, the freely accessible source code in the open source software (OSS) allows the end users to install it without additional purchases and gets/creates support from/for the community (Pearce, 2013).

The Linux operating system is perhaps the best project created from this open source paradigm. In the beginning, it was developed in 1991 by Linus Torvalds, a Finnish undergraduate student, during a computer science course. He released the source code and after some years that simple program became a full PC-based operating system, distributed over 90 countries. Even though its rapid growth, the reliability and quality were always high (Moon and Sproull, 2002).

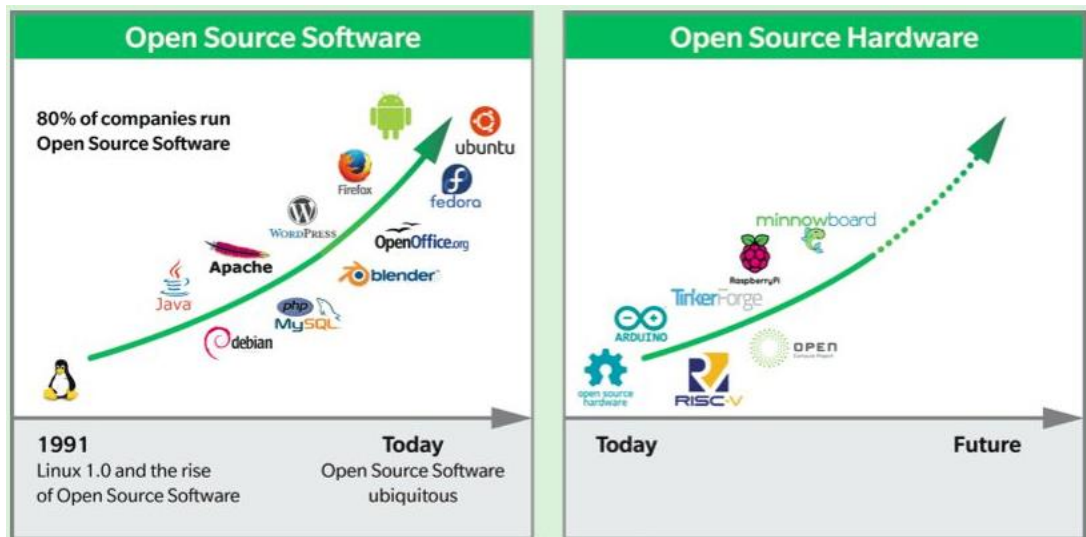


Figure 7: The rise of open software and the promising era of open hardware (Rambus website)<sup>5</sup>

Different authors stated that OSS, initially developed by unpaid volunteers, often has a higher quality than the proprietary closed source one (Bonaccorsi and Rossi, 2003). It is interesting to

<sup>5</sup> <https://www.rambus.com/blogs/1479-2/>

note that Microsoft products frequently suffer from technical drawbacks as bloat, lack of reliability, and security holes despite its undeniable developers' preparation. Indeed, the open source products can rely on a larger enthusiast community that makes it more efficient and adaptable (Kogut and Metiu, 2001). For instance, the Linux community is composed of thousands of programmers that are debugging, making suggestions and submitting code continuously. Another example of successfully mass collaboration includes the biggest online encyclopaedia: Wikipedia. It contains far more information and up-to-date contents than any conventional for-profit encyclopaedias. Looking forward, the monitoring technology for research purpose could take advantage from a similar path: sharing ideas on the open-source development of the hardware can bring to great results.

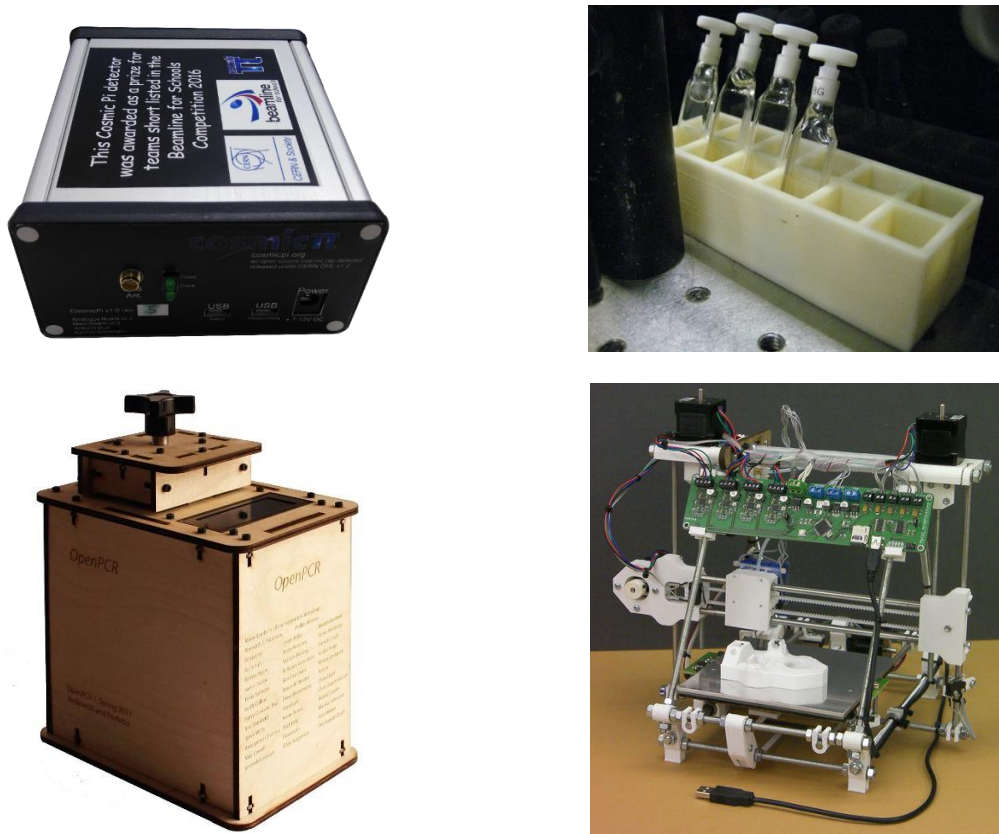


Figure 8: Cosmic Pi: Raspberry Pi-based cosmic ray detector (left-up); Parametric cuvette and vial rack (right-up)<sup>6</sup>; OpenPCR: DNA analysis (left-down); RepRap: self-replicating rapid prototype (right-down)<sup>7</sup>

<sup>6</sup> <https://www.thingiverse.com/thing:25080>

<sup>7</sup> <http://reprap.org/>

### 2.3.1 *Open-source technologies for Science*

Most experimental research projects require the purchase of expensive hardware and software, which in many cases has to be adapted for a specific purpose in the laboratory. In these regards, the open, collaborative principles of OSS can be easily transferred to scientific hardware design, making it extremely adaptable and inexpensive (Pearce, 2012). Nowadays, the options offered by the digital fabrication revolution, combining 3D printing with open-source microcontrollers, allows hobbyists, hackers and even researchers to custom-building their own equipment. Some of these successful examples are stated by Pearce's book on the open-source hardware for reducing research costs (Pearce, 2013): Cosmic PI (cosmic ray detector)<sup>8</sup>, pHduino (pH meter)<sup>9</sup>, Xoscillo (Oscilloscope)<sup>10</sup>, and OpenPCR (DNA analysis)<sup>11</sup>. One great example of a growing research community on open hardware is the Open Hardware Repository<sup>12</sup>. It was created by a group of electronics designers led by Javier Serrano, a CERN engineer, working in experimental physics laboratories with the aim of bring together hardware developers to share the results of their R&D activities (CERN Bulletin, 2011).

## 2.4 **Reviews of Microcontroller boards and Single-board computers**

In the last decade, we have seen a big growth in microcontroller boards and micro-computers. The modern era started with the diffusion of Arduino in the late 2000's (Figure 9): it changed the way electronics has been done, not only for hobbyists and enthusiasts but for professionals as well (Allan, 2017).

### 2.4.1 *Arduino board*

Briefly, Arduino is an open-source microcontroller based on a simple input/output board and on a development environment built on the Processing language<sup>13</sup> (Banzi, 2008). The main key to its success was the collaboration between users and the creation of a vast community. In 2003 it was

---

<sup>8</sup> <http://cosmicpi.org/>.

<sup>9</sup> <http://phduino.blogspot.com/>.

<sup>10</sup> <http://code.google.com/p/xoscillo/>.

<sup>11</sup> <http://openpcr.org/>.

<sup>12</sup> <http://www.ohwr.org/>

<sup>13</sup> <https://processing.org/>.

just a thesis project at the Interaction Design Institute of Ivrea, and nowadays it has become not only the most successful microcontroller board but also a sort of world's social network for hackers and makers (Rodriguez, 2014).

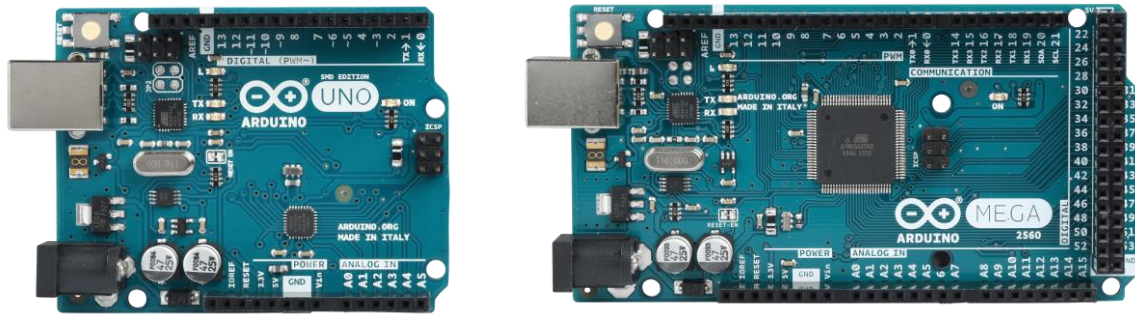


Figure 9: Arduino UNO (left) and Arduino MEGA (right)

#### 2.4.2 Internet of Things and Raspberry Pi

More recently, technological devices are increasingly seen as a way to communicate, from smartphones to smartwatches, and the need for a fast and efficient internet connection has become fundamental. The same is happening in the microcontroller board market. The Internet of Things (IoT) paradigm refers to the networking of everyday life devices with the web in order to send and receive information (Want et al., 2015). Before IoT, microcontrollers, as PC in the past, were mainly a way to control or automate, while nowadays they can collect and transmit information. On this side, the Raspberry Pi is rapidly growing in popularity. It is a board-size microcomputer developed in the United Kingdom with an integrated wi-fi antenna, Bluetooth, radio support, 4 USB channels and HDMI slot. The standard operative system is Rasbian, a Debian-based composed entirely of free-software, but other systems as Windows 10 or Android can be installed. This enables an excellent adaptability for many different users. As a consequence, Raspberry is the most significant trend in low-cost computers: in September 2016 reached the 10 million sold boards<sup>14</sup>.

<sup>14</sup> <http://fortune.com/2016/09/08/raspberry-pi-10-million/>

## 2.5 Review of low-cost sensors for structural monitoring

The parameters involved in structural monitoring include temperature, humidity and displacement. One of the main advantages of Arduino is the presence of an integrated analog-to-digital converter (ADC): it is a fundamental feature that converts an analog voltage on a pin to a digital number. This is crucial to interface low-cost analog sensors that measure light, temperature or sound with the digital world of computers. Furthermore, Arduino has an SPI (Serial Peripheral Interface Bus) and an I2C (Inter-Integrated Circuit) bus for digital sensors making easily possible to use the vast majority of the sensors currently on the market.

### 2.5.1 Texas Instruments' LM35 temperature device

The Texas Instruments' LM35 series<sup>15</sup> are temperature devices with a linearly proportional voltage output to degree Celsius. With a temperature range from  $-55^{\circ}\text{C}$  to  $150^{\circ}\text{C}$ , a typical accuracy at  $25^{\circ}\text{C}$  of  $\pm 0.4^{\circ}\text{C}$  and a maximum accuracy at  $25^{\circ}\text{C}$  of  $\pm 1.0^{\circ}\text{C}$ , this is one of the best solutions for very low-cost applications, especially considering that its price is lower than 1€. This integrated circuit operates from 4 V to 30 V with a scale factor of  $10\text{ mV}/^{\circ}\text{C}$ .

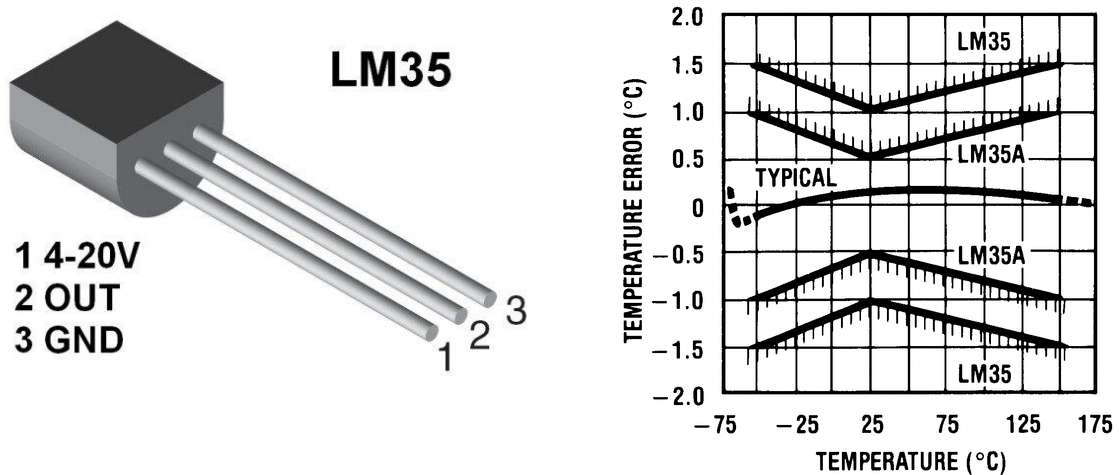


Figure 10: LM35 pin configuration (left) and diagram of maximum temperature error over operating temperature (right)

To sum up, the LM35 device has the following technical details:

- Analog device

<sup>15</sup> <http://www.ti.com/product/LM35>.

- Accuracy at 25°C:  $\pm 0.4^\circ\text{C}$
- Price: <1€
- Operating voltage: from 4 V to 30 V

### 2.5.2 Adafruit's DHT11 and DHT22 temperature and humidity sensors

The Adafruit's DHT11<sup>16</sup> and DHT22<sup>17</sup> are low-cost digital temperature and humidity sensors. They both use a capacitive humidity sensor and a thermistor to measure the surrounding air, giving back a digital signal on the data pin. Furthermore, it is important to note that they both read data every 2 seconds.

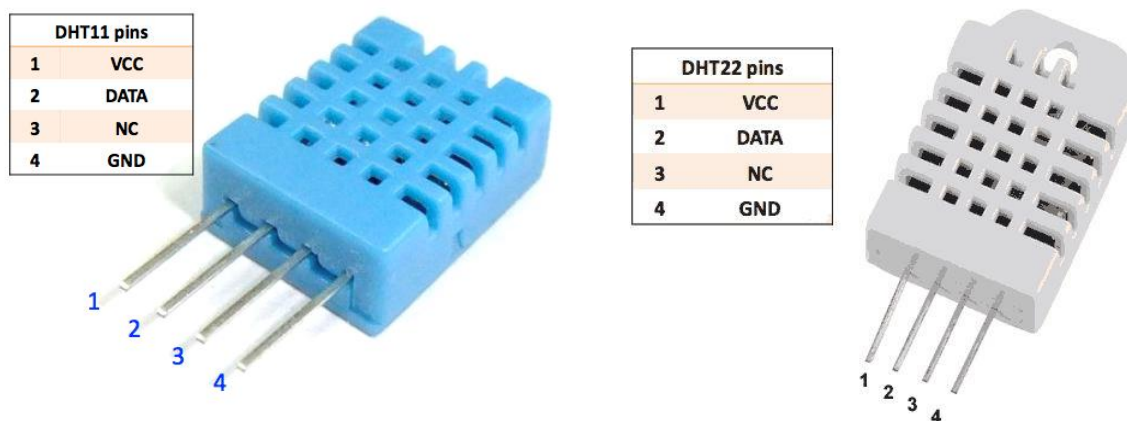


Figure 11: DHT11 pin configuration (left) and DHT22 pin configuration (right)

To sum up, respectively the DHT11 and the DHT22 devices have the following technical details:

- Digital sensors
- Temperature accuracy at 25°C:  $\pm 2^\circ\text{C}$  and  $\pm 0.2^\circ\text{C}$
- Humidity accuracy at 25°C:  $\pm 5\%$  RH and  $\pm 2\%$
- Price: 5€ and 10€
- Operating Voltage: 3-5.5V and 3.3-6V

It is clear that the much higher precision in DHT22 corresponds to a higher price.

<sup>16</sup> <https://www.adafruit.com/product/386>.

<sup>17</sup> <https://www.adafruit.com/product/385>.



### 2.5.3 Displacement control devices

In the last twenty-five years, SHM technologies have emerged as a new essential part of the civil engineering field. However, this is not a new concept. For thousands of years engineers, architects and masons have been controlling the ongoing structural performances of their buildings. Consequently, many low-cost devices for crack monitoring are already available on the market, as the crack width ruler, the tell-tale crack meter (Fig. 12), the digital electronic calliper or more precise techniques as the one based on the moiré patterns (Yen and Ratnam, 2011). Nevertheless, they all require continuous accessibility and periodic inspections. Otherwise, it is impossible to study the phenomenon evolution.

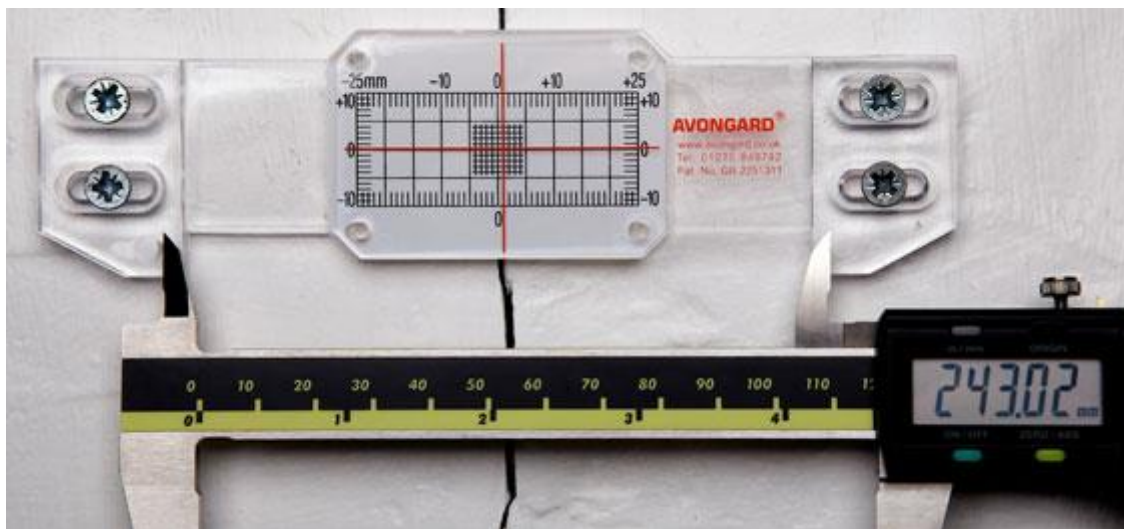


Figure 12: Tell-tale crack meter with a digital calliper<sup>18</sup>

More traditional techniques include the use of gypsum strips or some glued glass plates. These are a good solution only to check the short-time stability after some disasters such as flood, earthquakes or landslide otherwise not very meaningful for monitoring (Drdácký, 2005).

---

<sup>18</sup> <http://www.rstinstruments.com>

## 2.6 Final remarks

In this chapter, a state-of-the-art about SHM and low-cost open-source technologies was presented. Addressed issues include a review of monitoring strategies and components, a description of the main displacement transducers, the most important microcontrollers and single-board computer with particular attention to low-cost sensors.

As already stated, SHM is a highly valuable tool for the vulnerability assessment of historical constructions, but its wide diffusion is limited by the high costs. On the other hand, emerging technologies in the field of open hardware are particularly promising for low-cost monitoring applications. At the same time, the main limits of low-cost SHM are the lack of robust results and the need for high-precision data for a reliable monitoring. These two issues are the main focus of the next two chapters.

### 3 PREVIOUS EXPERIENCES IN STRUCTURAL LOW-COST MONITORING

This chapter describes what was previously done in SHM with the low-cost and open-source approach at UPC. It is important to note that both from the Arduino's community<sup>19</sup> and on the internet of things<sup>20</sup> (e.g. the system developed by Libellium for crack's monitoring) there are different good examples of low-cost monitoring systems. The systems analysed in this chapter are previous-research studies developed at UPC: the SAHC master thesis by Basto (Basto, 2015) and the master thesis in structural engineering by Martinez (Martínez Gil, 2017).

#### 3.1 First experience at UPC by Basto (2015)

As already stated, the purpose of this research is working just on the hardware on-site, namely the sensors and the data acquisition (DAS), and the communication systems. In order to better understand the different approaches, these elements are further divided as follow:

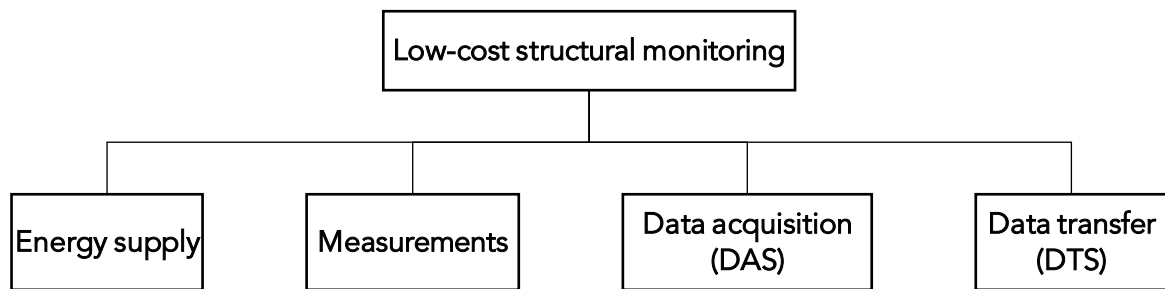


*Figure 13: Low-cost structural monitoring elements' diagram (Basto, 2015)*

These groups intend to enquire the main issues of a low-cost structural monitoring system:

- Energy supply: insurance of an adequate power supply to the electronic components with the desired features;
- Measurements: the system of sensors that are transforming a physical magnitude in an electronic signal (i.e. temperature, humidity and displacement);
- Data acquisition: the system able to collect data (i.e. the microcontroller);
- Data transmission: the system that can log and bring the information to the user.

---

<sup>19</sup> <http://forum.arduino.cc/index.php?topic=103679.0>.

<sup>20</sup> <http://www.libelium.com/development/waspmote/examples/sc-5-crack-sensor-reading/>.

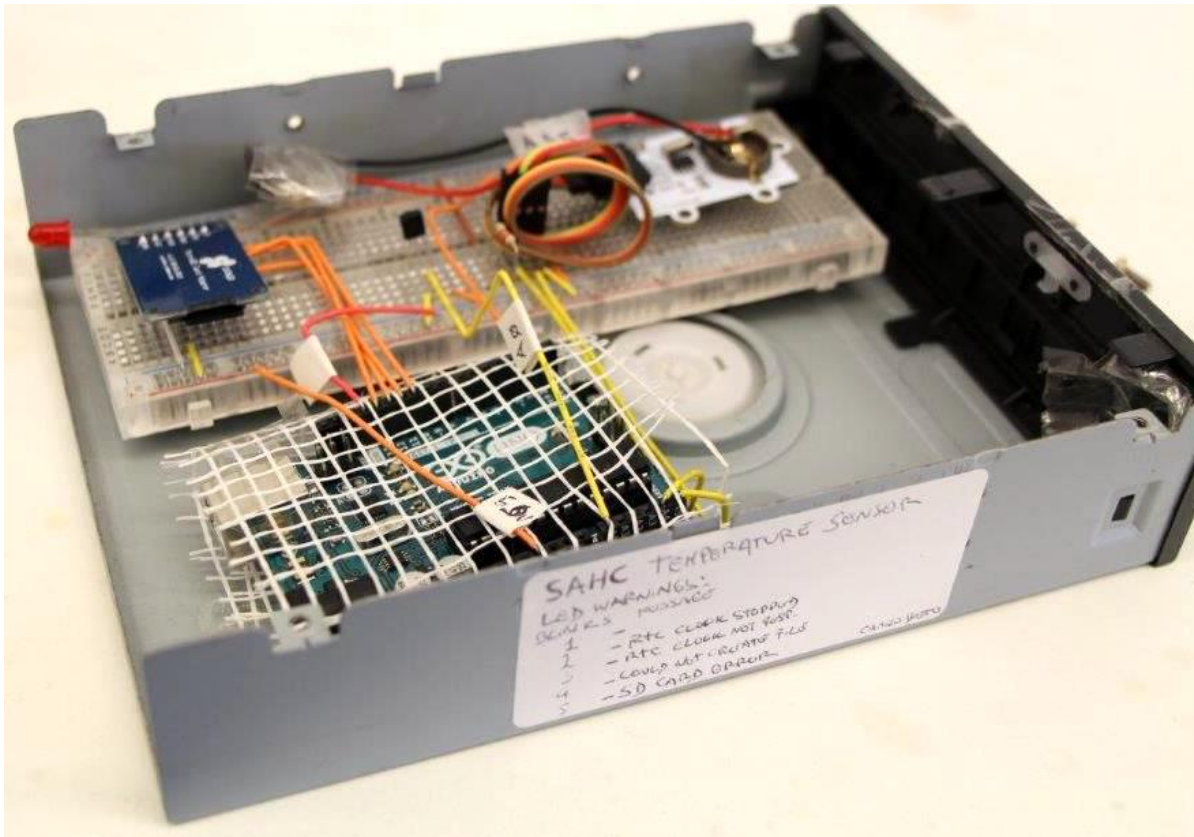


Figure 14: Basto's Temperature system (Basto, 2015)

Camilo Basto's SAHC master thesis (Basto, 2015) constitutes the first approach to low-cost structural monitoring, in which different possibilities were tested, and three different independent systems were built.

	Energy supply	Measurement	Data Transfer (DTS)
1	Solar Power	Temperature (LM35)	Storage in SD card - Inspection
2	Direct Current	LVDT (Solartron AX/5/S)	xBee Connection - PC
3	Battery and Current	Humidity (DHT22)	Bluetooth Connection - PC

Table 1: Systems built for the monitoring campaign (Basto, 2015)

The Data acquisition systems (DAS) are not listed because they were the same for every system: three Arduino UNO boards. Summarising, except for the temperature system (LM35) in the last step, the systems proposed by Basto were following the workflow in Figure 15.



Figure 15: System workflow according to Basto

It is important to note that the connection between the sensors and the DAS, and further the circuit on the DAS, were directly assembled on a breadboard (Fig 16). As explained below, this makes the systems difficult to be transported.

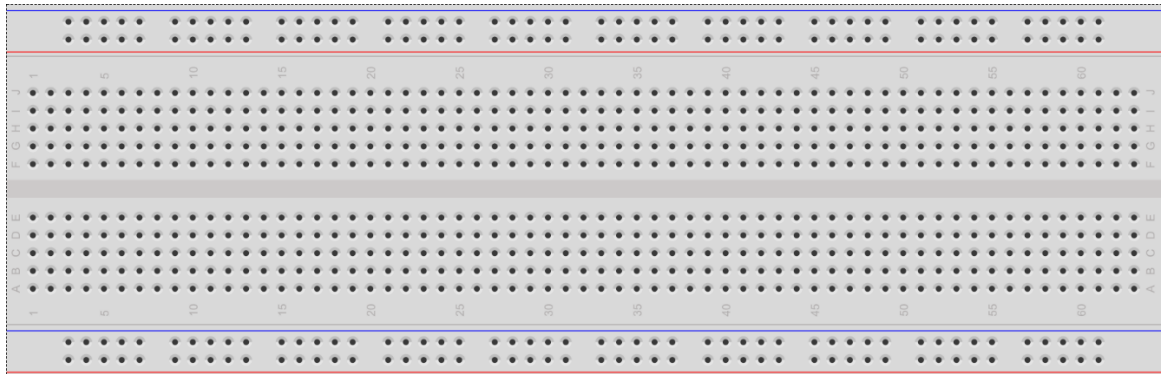


Figure 16: A solder-less breadboard

### 3.1.1 Results obtained

The results of the work were quite satisfactory, besides being the first application of a low-cost structural monitoring system. The work was also published in the Journal of Cultural Heritage (Basto et al., 2017) that acknowledged the novelty of its contribution to the field.

The systems were installed in the block B1 of the UPS's Northern campus in Barcelona. This case was chosen due to the clear activity of a crack on a non-structural element and its good accessibility, which provided the possibility of a continuous system's control. Furthermore, a computer was installed on-site in order to acquire data by xBee and Bluetooth. The remote access was also possible through the installation of Teamviewer software on the computer: this was important to check the sensor's activity.

The graph in Figure 17, shows the distribution of temperatures, recorded with an LM35 (blue-external temp.) and a DHT22 (purple-internal temp.), and humidity, recorded with the DHT22 (green-internal hum.).

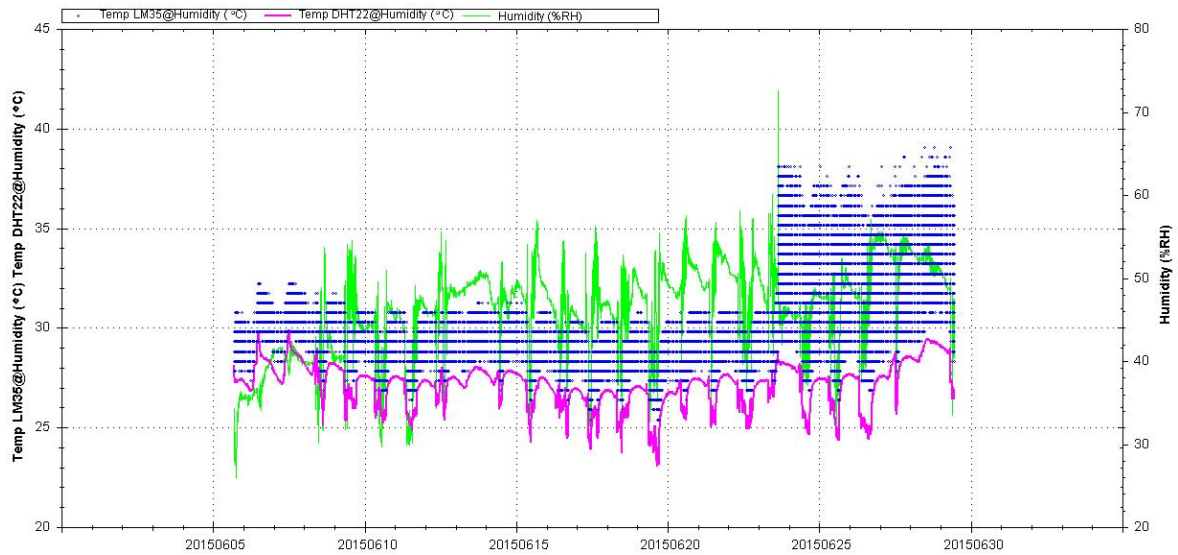


Figure 17: Internal temperature and humidity, and external temperature distribution over time (Basto, 2015)

On the other hand, the following graph concerns the evolution of the monitored crack, recorded with the LVDT (purple), and the internal temperature (blue) recorded with an LM35 installed on the LVDT's system over the same period.

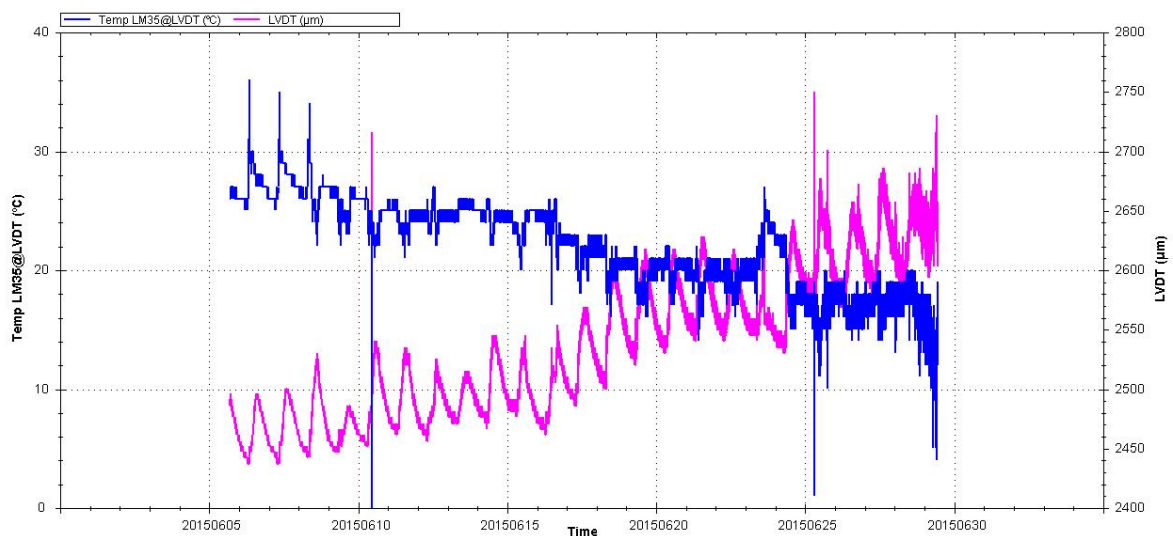


Figure 18: Displacement evolution and internal temperature distribution over time (Basto, 2015)

To finally clarify, the first graph refers to Temperature's and Humidity's systems, placed respectively outside and inside, while the second graph refers just to the LVDT's system placed inside.

### 3.1.2 *Comments*

As observed in Figure 17, the Temperature's system reports some drawback results. The LM35 sensor was probably affected by an extremely high electrical noise created by the solar panel. As the author stated (Basto, 2015), the solar panel was not working as expected due to positioning issues, producing less power than intended. Conversely, the DHT22 powered by a battery and after some days by direct current gave good results. The LVDT's system gave a quite clear signal in the beginning, but after a week it slowly becomes unclear. Again, the electrical noise was probably the cause, but in this case, the system was powered with direct current. Thus it is not so clear what generated this phenomenon. Overall, the expected day-night cycles were detected: in other words that means an outstanding resolution. Moreover, it is important to report that during the first days any data were recorded by the Temperature's system due to a faulty cable. This problem underlines the fragility of circuits built on a prototyping breadboard.

In conclusion, the results from the LVDT were very satisfactory as the one from the DHT22. The issues with the LM35 can be easily fixed with a printed circuit board.

## 3.2 **Second experience at UPC by Martinez (2017)**

The study presented in this paragraph was a part of the master thesis in Structural Engineering at UPC of Saray Martínez Gil (Martínez Gil, 2017). Compared to the system developed by Basto, this is a further step to cultural heritage deployment: a structural low-cost monitoring system was proposed to the parish of Santa Maria del Mar to study the evolution of two cracks. Regarding this aspect, an analysis of needs of the stakeholders involved is reported.

### 3.2.1 *Stakeholder involvement*

Particularly in structural monitoring for Cultural Heritage, it is important to identify all the people involved and interested in the monitoring project. Due to the complexity of the study, these stakeholders need to be active and up-to-date on the entire project's life-cycle. According to

Martinez (Martínez Gil, 2017) the way to make this activity and communication effective with both parties is to:

- Hold regular meetings;
- Send the information obtained - Conduct training sessions for non-professionals in the field;
- Conduct interviews and meetings with professionals in the field.

It is essential that the fundamental objectives of the monitoring system and the specific requirements are clearly identified and understood in this phase of initiation of the project, including any restrictions that may arise from the client. These decisions should come primarily from stakeholders but will need to be supported by a group of experts to identify realistic objectives and project requirements. Only after this process is understood, the client will be able to make the right decisions. The final objectives are:

- To monitor and characterise the structural behaviour
- To detect anomalies in the behaviour of the structures
- To identify and to know the causes of the problems
- To protect the goods of the Basilica during the operations carried out

### 3.2.2 System proposed by Martinez

The objective of Martinez was set-up a low-cost structural system in accordance with the principles of minimum intervention and minimum visual impact. For this reason, the size of the system had to be limited as much as possible. Consequently, a board that can be at the same time DAS and DTS was chosen: Arduino Yún has an additional processor equipped with a wi-fi connection. Figure 19 shows the entire set-up while Table 2 summarises the system's main component.

Energy supply	Measurement	DAS and DTS
Direct current	Temperature/Humidity: DHT11	Arduino Yún
	Displacement: Linear potentiometer	

*Table 2: Systems developed by Martinez for the deployment of low-cost structural monitoring in Santa Maria del Mar (Martínez Gil, 2017)*



The *Energy Supply* was chosen according to the specific needs of the case study. Continuous monitoring requires the acquisition of data 24 hours every day for several months or even years. As Martinez stated, batteries with great capacity require an amount of space that was not available in that area of the church. Due to the availability of the emergency current from the bell-tower, direct current was chosen.

Regarding the *Measurements*, data on internal temperature/humidity, external temperature and external light intensity were needed. Adafruit's DHT11 was chosen due to performance/cost ratio, and a simple photoresistor was selected to detect day/night cycles. Furthermore, displacement was measured with a linear potentiometer directly connected to the 5V line of Arduino Yún.

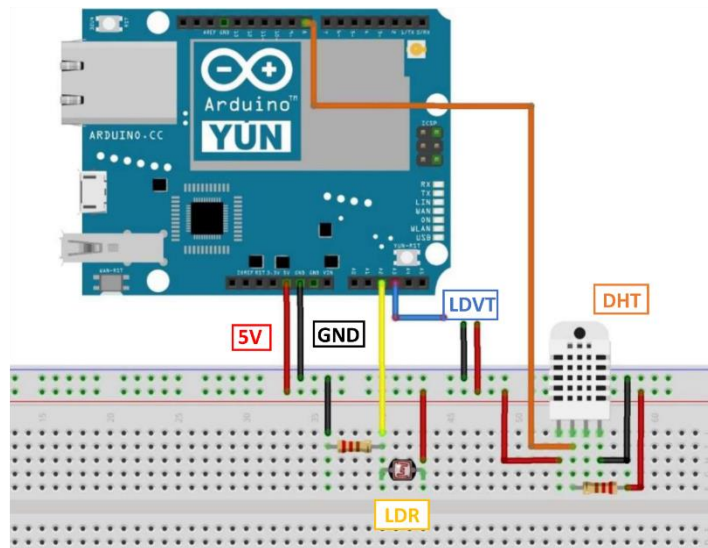


Figure 19: System developed by Martinez for the deployment of low-cost structural monitoring in Santa Maria del Mar (Martínez Gil, 2017)



Figure 20: The logo of SmartLab device

As already stated, the selected *Data Acquisition System* (DAS) had to allow sending and storing data to keep a small size to minimise the visual impact. For this reason, data acquisition and data

transmission systems are enclosed in the same device, the Arduino Yún. Indeed, Wi-Fi was chosen as the main way for sending the collected data in order to avoid the presence of a computer on-site. Finally, a receiver was implemented at the Department of Civil and Environmental Engineering of the Polytechnic University of Catalonia, the so called SmartLab device. It enables the reading and interpretation of results in real time.

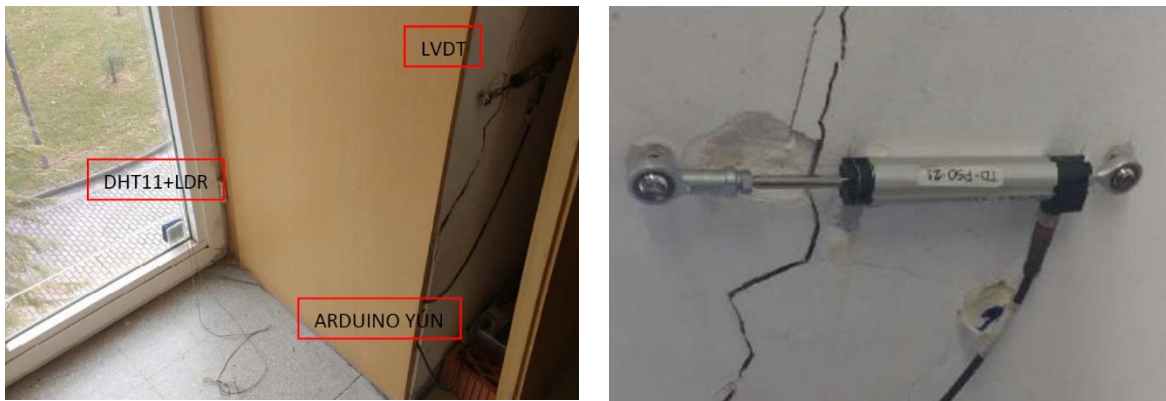
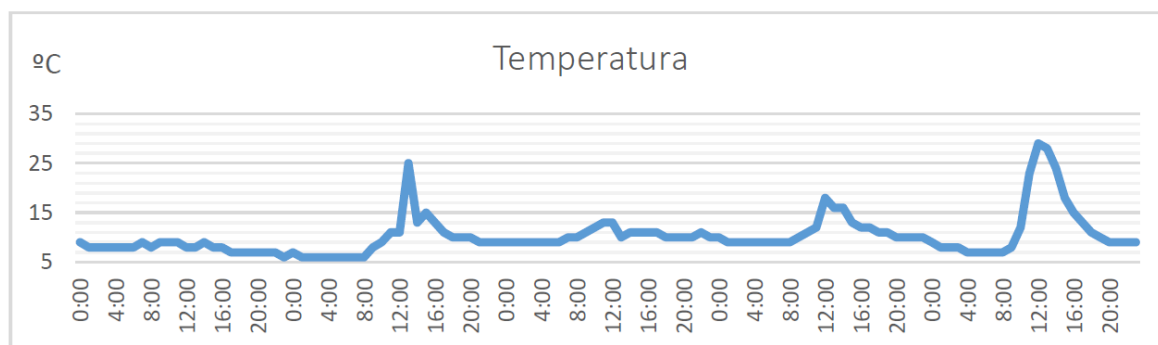


Figure 21: System installed by Martinez in the block B1 of the UPS's Northern campus (Martínez Gil, 2017)

### 3.2.3 Results obtained

In order to test the reliability of the system, it was installed in the block B1 of the UPS's Northern campus in Barcelona as Basto did. It was not casual the decision to take the same case study of the previous research: the behaviour was known and similar results were expected. In Figure 22 temperature and displacement recorded in five consecutive days in the winter are displayed. As already stated, other parameters were collected as humidity and light intensity but this analysis want to focus particularly in the results of the linear potentiometer.



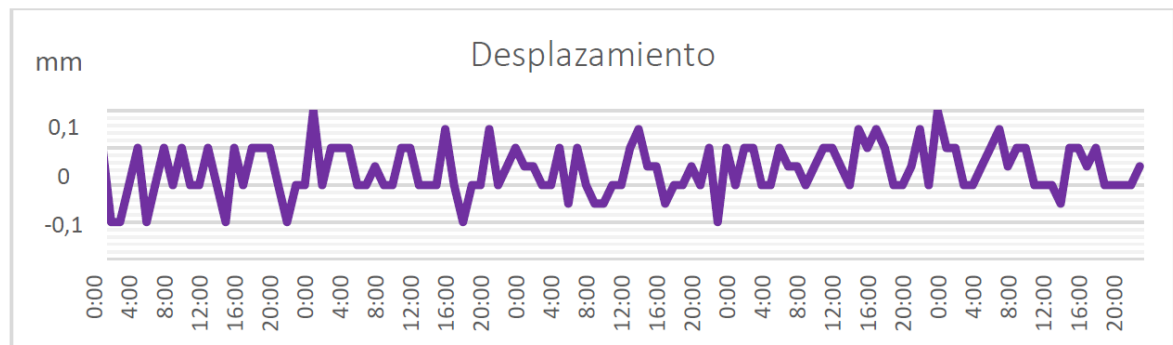


Figure 22: Temperature and displacement recorded between 25 January 2017 and 29 January 2017 by Martinez (Martínez Gil, 2017)

In figure 23 temperature and displacement recorded in five consecutive days in the spring are displayed.

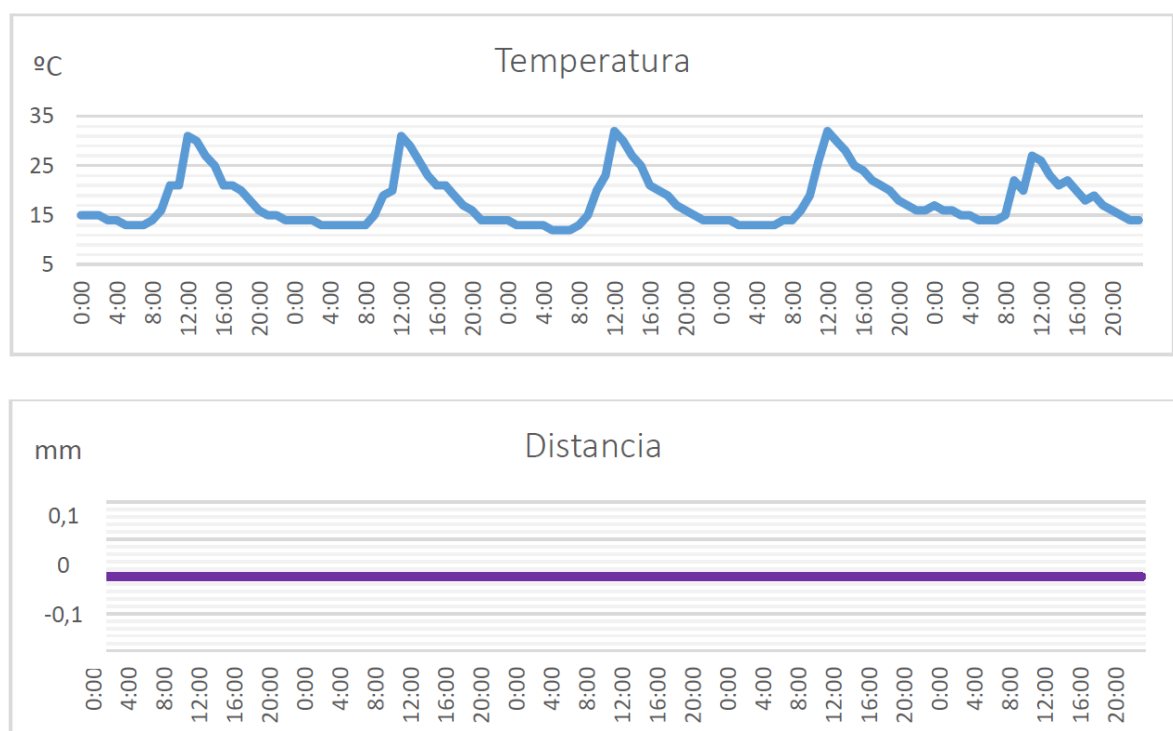


Figure 23: Temperature and displacement recorded between 11 April 2017 and 15 April 2017 by Martinez (Martínez Gil, 2017)

### 3.2.4 Comments

As observed in Figure 22 and 23, the results from the displacement measurement are very different compared to the ones of Basto (Figure 18). Certainly the LVDT deployed by Basto has a higher

resolution and precision compared to the Novotechnik TEX 50 used by Martinez. On the other hand, further analysis are needed to better comprehend why the results do not correspond to the expectations. Conversely, the novel approach proposed for the stakeholders involvement is really promising for future applications.

### **3.3 Lessons learned from previous experiences at UPC**

#### *3.3.1 Energy supply*

As already mentioned, the application of the solar panel in the system proposed by Basto was not really successful. The battery in the Humidity's system was just used for a period; then it was substituted with direct current. Indeed, the connection to the electrical grid through an AC adapter has so far been the better choice for both authors.

#### *3.3.2 Measures and sensors*

The analog temperature sensor by Texas Instrument, LM35, wasn't really suitable for high-precision applications. On the other hand, both the digital temperature sensors, DHT11 and DHT22, were good enough to catch the expected behaviour.

Moving to displacement sensors, the LVDT (Solartron AX/5/S) was deployed by Basto while the linear potentiometer (Novotechnik TEX 0050) was installed by Martinez. In the first case, the system was able to catch the expected day/night cycles quite accurately. Only after several days it started to be affected by noise. In the second case, the system was able to catch the overall crack opening but not the day/night movements. From these considerations on the results it seems that the first system had a better resolution than the second one.

#### *3.3.3 Data acquisition system (DAS)*

In both cases a 10-bit ADC was employed, limiting especially the resolution of displacement sensors. On the other hand, the Arduino UNO and the LVDT proposed by Basto didn't really suffered from this drawback. Conversely, the application of Arduino Yún and a linear potentiometer clearly conditioned by the low resolution of the system.

#### 3.3.4 *Data transmission system (DTS)*

One of the significant limitation of the DTS proposed by Basto was the need of a computer on-site. In both cases, Bluetooth and the xBee technologies needed a closed receiving system to exchange information. This aspect can be problematic especially in a cultural heritage building, where the space available is often limited. On the other hand, they remain a very valuable tool for short connection with the system through tablet or smartphone.

Conversely, the DTS proposed by Martinez focussed on wi-fi connection. Particularly, through the implementation of the SmartLab device, the data transmission with a remote server was much easier. The connection was made directly from the Arduino Yún's wi-fi.



## 4 IMPLEMENTATION OF A NEW LOW-COST STRUCTURAL MONITORING SYSTEM

The main aim of this work it is to develop a reliable system, understanding the data resolution and error, for the static structural monitoring of Santa Maria del Mar Church. Consequently, it is important to understand the parameters that influence the overall reliability of a low-cost system. This chapter describes the experience in the laboratory of Camins Makers<sup>21</sup> during dissertation's period. It reports the selection process of the components, the set-up of the new system and its testing with a reference device. Firstly, to understand better the problem, some basic concepts of metrology, electronics and signal processing have to be recalled.



Figure 24: Implementation of a new low-cost structural monitoring system

### 4.1 Useful concepts of metrology, electronics and signal processing

During the research of the right components for this application, a vast array of product specifications was founded. In order to select the best cost-performance ratio, some parameters have to be chosen to allow a direct comparison. Unfortunately, understanding how the different parameters affect each other is a somehow complex task. Further investigations on some basic concepts of electronics and sensor specifications were needed.

#### 4.1.1 Accuracy, Precision, Sensitivity and Resolution

According to the International vocabulary of metrology or IVM (Joint Committee for Guides in Metrology, 2012), the *accuracy* of measurement is the “closeness of agreement between a measured quantity value and the true quantity value”. In other words, it is the amount of uncertainty of a measured value with respect to a standard value. For example, if a displacement of 3.00mm is imposed to a linear potentiometer connected to a DAS that reads 4.00mm, the

---

<sup>21</sup> <http://caminsmakers.upc.edu/>.

measurement is not accurate. It is important to underline that according to IVM, measurement accuracy is not a numerical value.

On the other hand, measurement *precision* is the “closeness of agreement between indications or measured quantity values obtained by replicate measurements on the same or similar objects under specified conditions” (Joint Committee for Guides in Metrology, 2012). In other words, it is the reproducibility of a steady state signal measured many times. Using the example above, if the potentiometer reads 4.00mm for 10 times, the measurement is very precise. Moreover, precision is expressed numerically as the standard deviation, the variance, or the coefficient of variation (Joint Committee for Guides in Metrology, 2012).

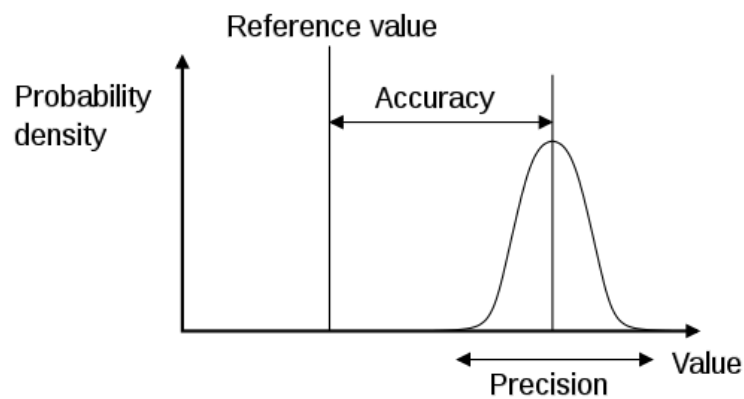


Figure 25: Difference in Accuracy and Precision<sup>22</sup>

The *sensitivity* of a measuring system is the “quotient of the change in an indication of a measuring system and the corresponding change in a value of a quantity being measured” (Joint Committee for Guides in Metrology, 2012). In other words, it is the smallest absolute amount of change that can be detected by a measurement.

Measurement *resolution* is the “smallest change in a quantity being measured that causes a perceptible change in the corresponding indication” (Joint Committee for Guides in Metrology, 2012). In other words, it is the smallest reliable measure that a system can make. Often it directly depends on electrical noise or friction.

<sup>22</sup> [https://en.wikipedia.org/wiki/Accuracy\\_and\\_precision](https://en.wikipedia.org/wiki/Accuracy_and_precision).



Resolution is one of the most important specifications in this application. Without a sufficient resolution, the system will not provide reliable measurements, while the use of an over performing sensor can be an unnecessary cost.

#### 4.1.2 Analog-to-Digital converter (ADC)

In order to interface an analog device (e.g. temperature sensors, position sensors, strain gauges, etc.) with a digital circuit, an analog-to-digital converter (ADC) is needed. It translates an analog signal into a series of binary numbers, each one proportional to the level measured in a given moment. Commonly, the digital strings generated by the ADC are sent to a microcontroller or a microprocessor, where they are processed (Scherz, 2000).



Figure 26: Analog-to-Digital converts: 12-bit Adafruit's ADS1015 (left); 10-bit Maxim Integrated's MAX177 (center); 16-bit Texas Instruments' DAC8830 (right)

The ADC selection is based on various system requirements such as resolution, power source, conversion speed or physical size (Mancini, 2002). Firstly, the ADC must have an adequate number of bit to obtain the desired results. The ADC resolution is calculated by the following expression:

$$\text{ADC resolution} = 2^N \quad (1)$$

$N$  is the number of significant bits contained in the ADC. It is important to clarify that the word *bits* will be used in two different ways: *binary bits* are zeros and ones in the binary strings, while the significant bits are a characteristic of the ADC. Most Arduino boards have an analog resolution of 10-bit. Consequently, the number of binary bits is equal to:

$$\text{Arduino UNO binary bits} = 2^{10} = 1024 \quad (2)$$

1024 represents the number of the different analog levels that the microprocessor can use. The following example is an 8-bit converter, so  $2^8 = 256$  binary bits.

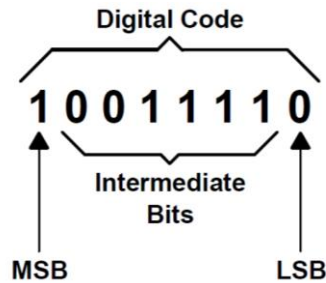


Figure 27: Significant bits (Mancini, 2002)

The voltage value of a single significant bit is called the least significant bit (LSB). In the case of Arduino UNO, the LSB is equal to:

$$\text{LSB} = \text{FSV} / (2^N - 1) = 5 \text{ [V]} / 1023 = 4,89 \text{ [mV/bit]} \quad (3)$$

FSV is the full-scale voltage of the converter. In an ADC, the LSB is the maximum voltage change required for a one-bit output change (Mancini, 2002). Typically, the conversion speed is not critical in a structural static monitoring application, since changes occur at slow rates. As already stated in paragraph 2.4.1, Arduino has an internal ADC with a resolution of 10-bit. The only exemption is Arduino DUE that has a 12-bit resolution.

#### 4.1.3 Overview of noise analysis in electronic circuits

A basic understanding of noise sources and analysis is required to develop a suitable instrument. Generally speaking, noise is a random unwanted part of the signal analysed (Leach, 1994). It can be divided in inherent noise and interference noise (T. C. Carusone, D. A. Johns, 2012).

Inherent noise can be partially filtered, but not completely removed since this noise is due to fundamental properties of the circuits (T. C. Carusone, D. A. Johns, 2012). In some application increasing the power supply can significantly increase the signal, reducing the inherent noise. On the contrary, interface noise is caused by interactions between different part of the circuit and the external environment. It can be reduced by careful circuit layout and wiring. It generally has a normal distribution and can be easily filtered by averaging.

In conclusion, understanding the source of noise is complex and time demanding. One of the main issues with the Arduino's ADC is the voltage instability, particularly high if the board is powered with USB cable<sup>23</sup>. The unstable output voltage supply results in an unstable signal from the analog sensors fed with that line. One way to overcome this problem is using the internal 1.1V reference (not present on Arduino DUE) or alternatively use an external linear power supply.

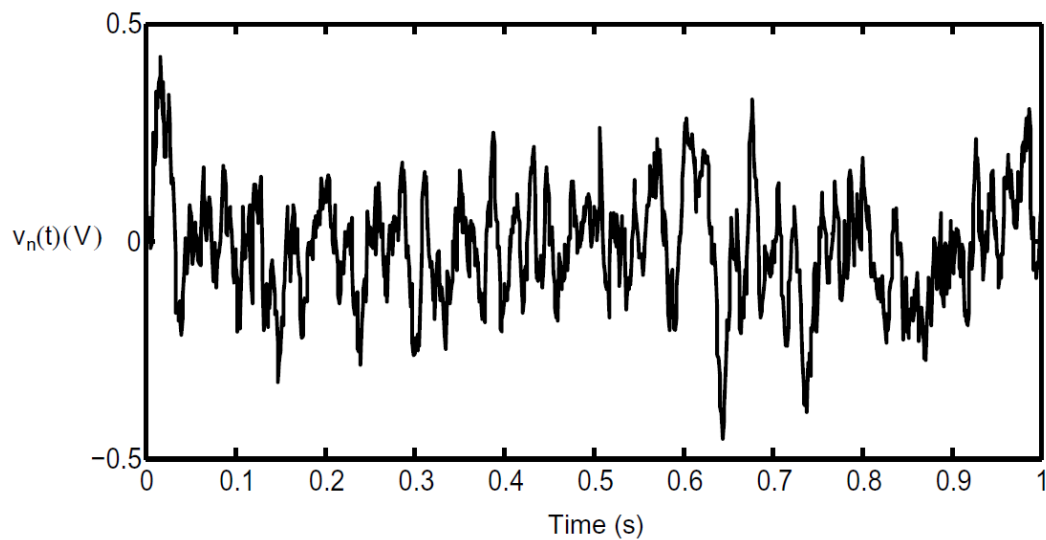


Figure 28: Voltage noise signal in the time domain (T. C. Carusone, D. A. Johns, 2012)

## 4.2 Components selection

One of the main issues in the systems proposed by Basto and Martinez was the measurement resolution regarding the displacement sensors. In the first case, the expected behaviour was cached from the beginning with some drawbacks related to electrical noise in the end. In the second case, the limitations given by some components were bigger. In Martinez's system, no direct correlation with the day-night cycles was found due to analog resolution issues with the DAS. Consequently, it is of particular importance to focus on the DAS selection before, and then to choose the rest as a consequence.

### 4.2.1 DAS selection

Table 3 shows the recently most popular boards available on the market.

---

<sup>23</sup> Many examples on <https://forum.arduino.cc>



Arduino UNO

Arduino Yún

Arduino DUE

BeagleBone  
Black WirelessRaspberry Pi  
3

Price	20.00 €	65.00 €	36.00 €	70.00 €	40.00 €
Summary	<p>The UNO is the best board to get started with electronics and coding</p> <p>Perfect board for connected systems and IoT projects</p> <p>Based on a 32-bit ARM core microcontroller. It is the board for powerful large-scale projects</p> <p>Next-gen, ARM-based, hardware Linux board</p> <p>Single board Linux computer from the UK</p>				
CPU	ATmega328P	ATmega32u4 and Atheros AR9331	Atmel SAM3X8E ARM Cortex-M3 CPU	Octavo Systems OSD3358 1GHz ARM Cortex-A8	Quad Core 1.2GHz Broadcom BCM2837 64bit CPU
Speed	16 MHz	16 & 400 MHz	84 MHz	1GHz	1.2GHz
Analog pin	6	12	12	7	none
ADC resolution	10-bit	10-bit	12-bit	12-bit	none
Digital I/O Pin	14 (6 PWM)	20 (7 PWM)	54 (12 PWM)	65 GPIO (8 PWM)	40 GPIO
Digital I/O power	5V	5V	3.3V	3.3V	3.3V

Table 3: Microcontrollers comparison

As explained in the paragraph 4.1.2, the ADC resolution is particularly important for this application. The BeagleBone Black has a very powerful CPU and shows outstanding connectivity features, but the ADC performance does not justify the higher price. The Raspberry Pi cannot be used directly as a DAS since it does not have any ADC on the board. On the other hand, 10-bits of resolution are enough only with a short-range sensor. The linear potentiometer (Novotechnik TEX 0050) applied in the system proposed by Martinez (MTZ) has a range (R) of  $\pm 25\text{mm}$  and an overall range of 50mm. The global resolution of the system in term of mm is equal to:

$$\text{Resolution MTZ} = \text{LSB} \cdot \frac{R}{V_{\text{ref}}} = \frac{R}{(2^N-1)} = 50 [\text{mm}] / 1023 = 0,05 [\text{mm}] \quad (4)$$

This means that the smallest measurement theoretically achievable by the system is equal to 0,05mm. In theory, because it does not take into account the accuracy of the DAS, the presence of electrical noise in the circuit and the voltage stability, particularly significant for potentiometers. It is clear that the use of a smaller range, like the one employed by Basto (BST), guarantees a vast improvement in term of resolution. The Solartron AX/5/S has a range of  $\pm 5\text{mm}$  and an overall range of 10mm. Consequently, the global resolution of the system in term of mm is equal to:

$$\text{Resolution BST} = \text{LSB} \cdot \frac{R}{V_{\text{ref}}} = \frac{R}{(2^N-1)} = 10 [\text{mm}] / 1023 = 0,01 [\text{mm}] \quad (5)$$

Looking at the Arduino UNO and Arduino Yún's datasheets (respectively ATmega328P and ATmega32u4), an absolute accuracy of  $\pm 2\text{LSB}$  is reported. It is defined in the datasheet as "the maximum deviation of an actual (unadjusted) transition compared to an ideal transition for any code. This is the compound effect of offset, gain error, differential error, non-linearity, and quantization error"<sup>24</sup>.

In other words, every sample is affected by an error of four counts of the 0-1023 count range. Unfortunately, the datasheet specifies just this Absolute Resolution that, according to paragraph 4.1.1, is the measurement accuracy of the Arduino's ADC, for any given sample reading. As previously calculated, the LSB for 10-bit resolution is equal to 4,89 [mV/bit] and 2 LSB are equal to 9,78 [mV/bit]. Moving from volt to mm:

---

<sup>24</sup> [http://www.atmel.com/images/Atmel-8271-8-bit-AVR-Microcontroller-ATmega48A-48PA-88A-88PA-168A-168PA-328-328P\\_datasheet\\_Complete.pdf](http://www.atmel.com/images/Atmel-8271-8-bit-AVR-Microcontroller-ATmega48A-48PA-88A-88PA-168A-168PA-328-328P_datasheet_Complete.pdf).

$$\text{Accuracy MTZ} = \pm 2\text{LSB} \cdot \frac{R}{V_{\text{ref}}} = \pm 9,78 \text{ [mm]} \cdot \frac{50 \text{ [mm]}}{5000 \text{ [mV]}} = \pm 0,10 \text{ [mm]} \quad (6)$$

$$\text{Accuracy BST} = \pm 2\text{LSB} \cdot \frac{R}{V_{\text{ref}}} = \pm 9,78 \text{ [mm]} \cdot \frac{10 \text{ [mm]}}{5000 \text{ [mV]}} = \pm 0,02 \text{ [mm]} \quad (7)$$

Another important issue that will be addressed in the next chapter is the stability of the reference voltage ( $V_{\text{ref}}$ ) and in general the fluctuation in the applied voltage ( $V_{\text{in}}$ ). In conclusion, it is clear that MTZ accuracy was insufficient to guarantee the potentiometer's resolution of 0,01mm, while the little LVDT's range of BST helped to keep a good resolution and accuracy. Nevertheless, as it will be explained in the next paragraph,  $\pm 5\text{mm}$  is a too small range for Santa Maria del Mar application. Therefore, the only way to increase the overall resolution is deploying an ADC with 12-bit resolution. Arduino DUE was consequently chosen as DAS.

#### 4.2.2 Sensors selection: displacement

As it was explained in the previous paragraph, the displacement measurement is the most complex issue. For this reason, it will be the first one addressed, while the environmental parameters (as temperature and humidity) will be explained later.

The first parameter to be considered is the range of measurement needed. Unfortunately, this parameter may vary considerably depending on the type of crack: from  $\pm 0,6 \text{ mm}$  (Lorenzoni et al., 2015) to several millimetres in the case the crack is a thermal joint in the masonry wall. Consequently, the minimum measurement range is equal to  $\pm 10\text{mm}$ . Potentiometers have a larger measurement range than LVDT. Secondly, the sensor's output that DAS has to read is a voltage. LVDT needs an alternate current (AC) on the main coil, so it cannot be fed directly by Arduino since its output is a direct current (DC). The simpler system is the Linear Potentiometer: it works with DC, and the output signal is the voltage. The last parameter considered is the precision: an acceptable value is 0,01mm. In this case, the day-night cycles can be easily identified.

Finally, the LSB of the Arduino Due (12-bit ADC) and the overall resolution of the system are calculated. In the following expressions, just the measurement range ( $R$ ) of the Novotechnik TEX 0050 potentiometer is reported:

$$\text{LSB 12-bit} = \text{FSV} / (2^{12} - 1) = 3,3 \text{ [V]} / 4095 = 0,81 \text{ [mV/bit]} \quad (8)$$

$$\text{Resolution 12-bit} = \text{LSB} \cdot \frac{R}{V_{\text{ref}}} = \frac{R}{(2^{12} - 1)} = 50 \text{ [mm]} / 4096 = 0,012 \text{ [mm]} \quad (9)$$

As in the previous case of Arduino UNO and Yún, the DUE's maximum-minimum and common variation of LBS are reported in the SAM3X datasheet. The performance is measured with the

Integral Nonlinearity method (INL) and the Differential Nonlinearity method (DNL). The worst outcome is obtained with the INL: maximum variation of  $\pm 2,2\text{LSB}$  and typical variation of  $\pm 1\text{LSB}$ .

$$\text{Accuracy 12-bit} = \pm 2,2\text{LSB} \cdot \frac{R}{V_{\text{ref}}} = \pm 1,77 \cdot \frac{50 [\text{mm}]}{3300 [\text{mV}]} = \pm 0,027 [\text{mm}] \quad (10)$$

Accuracy has to be considered as the most disadvantageous value. In the Table 4, the parameters used in the selection of the displacement sensors are summarised:



		
	<b>LVDT: Solartron AX/5/S</b>	<b>Potentiometer: Novotechnik TEX 0050</b>
<b>Range [mm]</b>	$\pm 5$	$\pm 25$
<b>Input/output signal</b>	AC in the primary coil and DC in secondary coils/DC	DC
<b>Difficulty of circuit design</b>	Moderate/High <sup>25</sup>	Low
<b>Cable length sensitivity</b>	High (Dunnicliff, 1993)	Low (Dunnicliff, 1993)
<b>Sensor's accuracy [mm]</b>	0,005 <sup>26</sup>	0,01 <sup>27</sup>
<b>System LBS [mV/bit]</b>	1,22 (it is related just to the DAS)	
<b>System resolution [mm]</b>	0,002	0,012
<b>System accuracy [mm]</b>	$\pm 0,005$ or sensor accuracy	$\pm 0,027$ or sensor accuracy
<b>Cost</b>	Moderate (approx. 600€) <sup>28</sup>	Low (approx. 150€) <sup>29</sup>

Table 4: Displacement's sensors comparison

<sup>25</sup> In order to connect the LVDT with a microcontroller as Arduino a series of components is needed. In order, from the DC power supply to the Readout system: AC carrier generator, amplitude regulator, LVDT, demodulator, amplifier (Dunnicliff, 1993).

<sup>26</sup> Solartron AX/5/S datasheet.

<sup>27</sup> Novotechnik TEX 0050 datasheet.

<sup>28</sup> Estimation by <http://www.motionusa.com>.

<sup>29</sup> Estimation by <https://www.distrelec.ch>.

In conclusion, a linear potentiometer was chosen as a displacement sensor. Particularly, due to availability in the laboratory, the Novotechnik TEX 0050 was deployed. As already stated, it was the same device used in the system proposed by Martinez: in doing so, a better understanding of Martinez's results was possible.

On the other hand,  $\pm 0,03$  mm of accuracy out of a sensor's accuracy of 0,01 mm was not a satisfactory result, moreover the entire range of  $\pm 25$  mm was not needed. Consequently, it is possible to shorten the measurement range by supplying the sensor with the 5V line and keep 3.3V as a reference voltage for Arduino DUE. In other words, 3.3v corresponds to 4095 on the ADC and 33 mm on the sensor. As a consequence, the new system specifications are:

$$\text{Resolution 12-bit} = \frac{FSV}{(2^{12}-1)} \cdot \frac{R}{V_{\text{ref}}} = 3,3[V]/4095 \cdot 50[\text{mm}]/5[V] = 0,00806 [\text{mm}] \quad (11)$$

$$\text{Accuracy 12-bit} = \pm 2,2\text{LSB} \cdot \frac{R}{V_{\text{ref}}} = \pm 1,77 \cdot \frac{50 [\text{mm}]}{5000 [\text{mV}]} = \pm 0,0177 [\text{mm}] \quad (12)$$

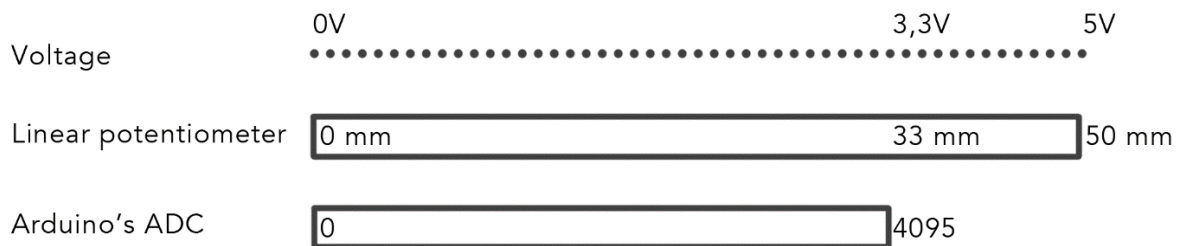


Figure 29: Linear potentiometer's data correspondence with Arduino DUE

#### 4.2.3 Sensors selection: temperature and humidity

As shown in paragraph 3.3.3, the temperature sensor that gave the best performance was the DHT22. To confirm these results, further experiments in the Camins Maker laboratory were done using the DUE system.

In the first experience, the Texas Instrument's LM35 and the Adafruit's DHT11 and DHT22 were installed on the same Arduino DUE board. The sampling period was equal to 600 seconds and 1 sample every 3 seconds was recorded. Roughly at second 100, an external excitation was imposed through breathing on the sensors.



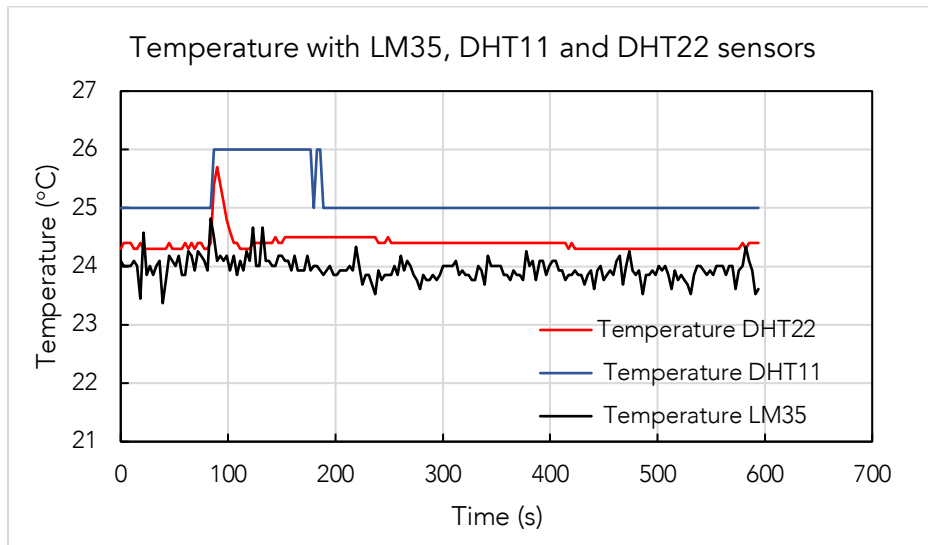


Figure 30: Temperature sensors test

It is clear that the low accuracy of DHT11 ( $\pm 2^{\circ}\text{C}$ ) make the device unusable. On the other hand, the results from LM35 ( $\pm 0,4^{\circ}\text{C}$ ) and DHT22 ( $\pm 0,2^{\circ}\text{C}$ ) are similar, but the first one shows a very unstable behaviour. It is important to note that DHT11 and DHT22 are digital sensors, while LM35 is an analog sensor and consequently suffers from the unstable input voltage and electrical noise.

The graph in Figure 31 reports the humidity sensors test. The sensors are the same as the ones used in the previous graph. Indeed, DHT devices can read temperature and humidity simultaneously.

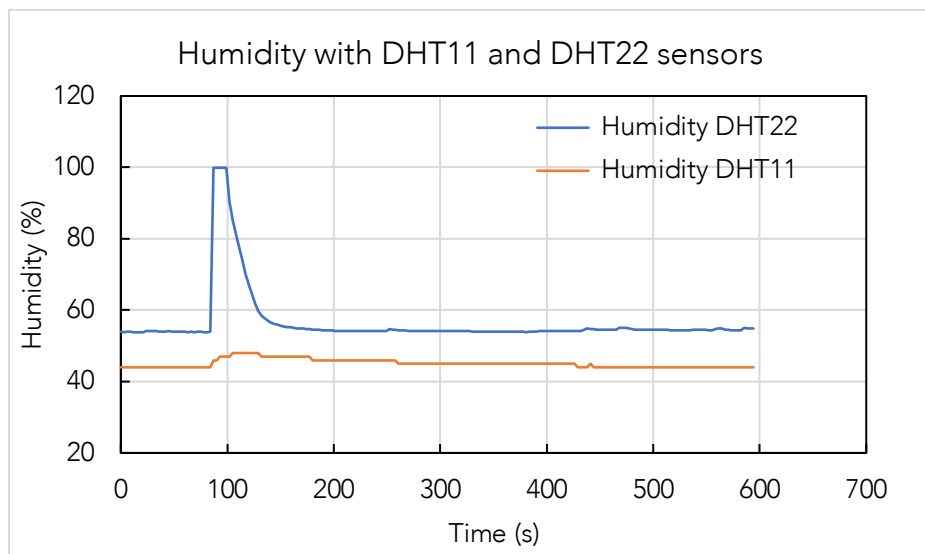


Figure 31: Humidity sensors test

In this case, the difference between DHT11 and DHT22 is even more clear. Especially the short external excitation is almost ignored by the DHT11.

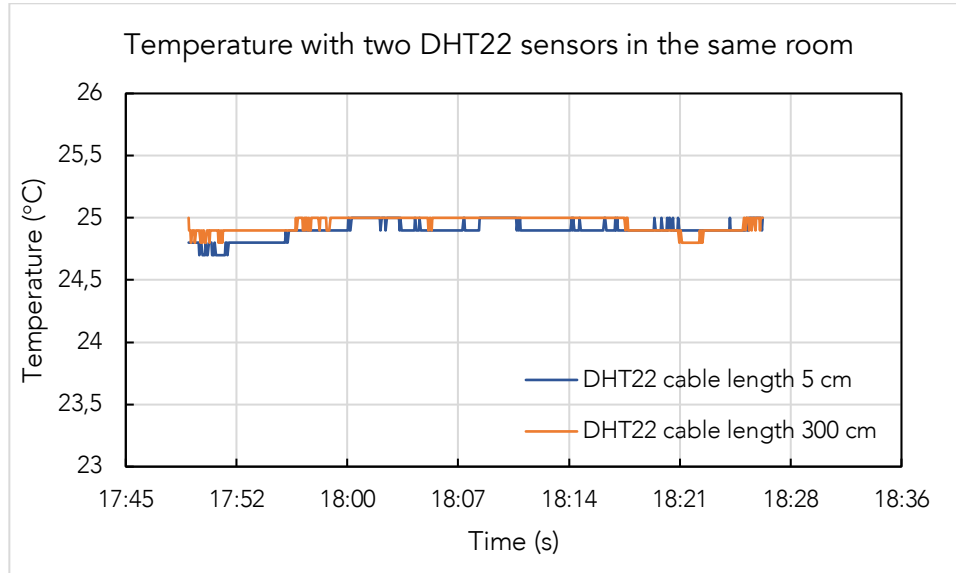


Figure 32: DHT22 cable length sensitivity

The Figure 32 shows the sensitivity to the cable length of the DHT22. Since these are digital devices, the measured physical magnitude is directly converted into a digital signal within the sensors. As expected, the digital data transmission is not sensitive to cable length. The parameters used to select the temperature and humidity sensors are summarised:



LM35



DHT11



DHT22

Type of sensor	Analog	Digital	Digital
Temperature accuracy	$\pm 0.4^{\circ}\text{C}$	$\pm 2^{\circ}\text{C}$	$\pm 0.2^{\circ}\text{C}$
Humidity accuracy	None	$\pm 5\%$	$\pm 2\%$
Operating voltage	From 4 V to 30 V	From 3 V to 5.5V	From 3.3 V to 6 V
Cost	Very low (<1€)	Low (approx. 5€)	Low (approx. 10€)

Table 5: Temperature's sensors comparison

Finally, the DHT22 device was selected, despite the higher price. It was to be preferred the higher reliability of the data than a few euros saved, especially after the limitations demonstrated by Basto with LM35.

#### 4.2.4 *Data transmission system (DTS) and energy supply*

One of the main issues related with continuous monitoring is the data transmission. Through the connection between Raspberry Pi and SmartLab device, the visualisation of the real-time data can be done directly by a remote access to the cloud. Another important issue is the continuity of the power supply. According to Martinez (Martínez Gil, 2017), the best solution is the connection with the emergency electrical grid of the bell-tower.

#### 4.2.5 *Final remarks*

Firstly, it is important to point out that the main limiting factor up to this stage is the accuracy, lowered by the integral nonlinearity (INL) of the Arduino DUE's ADC. In the calculations, the worst nonlinearity factor was considered, but an optimal voltage supply can bring back INL to the standard value of  $\pm 1\text{LBS}$ , that is  $\pm 0,012\text{ mm}$ . Therefore, it is necessary to test the system with a reference device as a Displacement Transducer Calibration Device and to obtain some clear experimental data.

In conclusion, the cost of the system is equal to 404€ and is composed by the following components:

- 2 linear potentiometers (Novotechnik TEX 50):  $2 \times 150\text{€} = 300\text{€}$
- 1 Arduino DUE: 36€
- 1 Raspberry Pi: 40€
- 1 Real time clock: 3€
- 2 Adafruit's DHT22:  $2 \times 10\text{€} = 20\text{€}$
- Some cables, LDR and resistors: about 5€

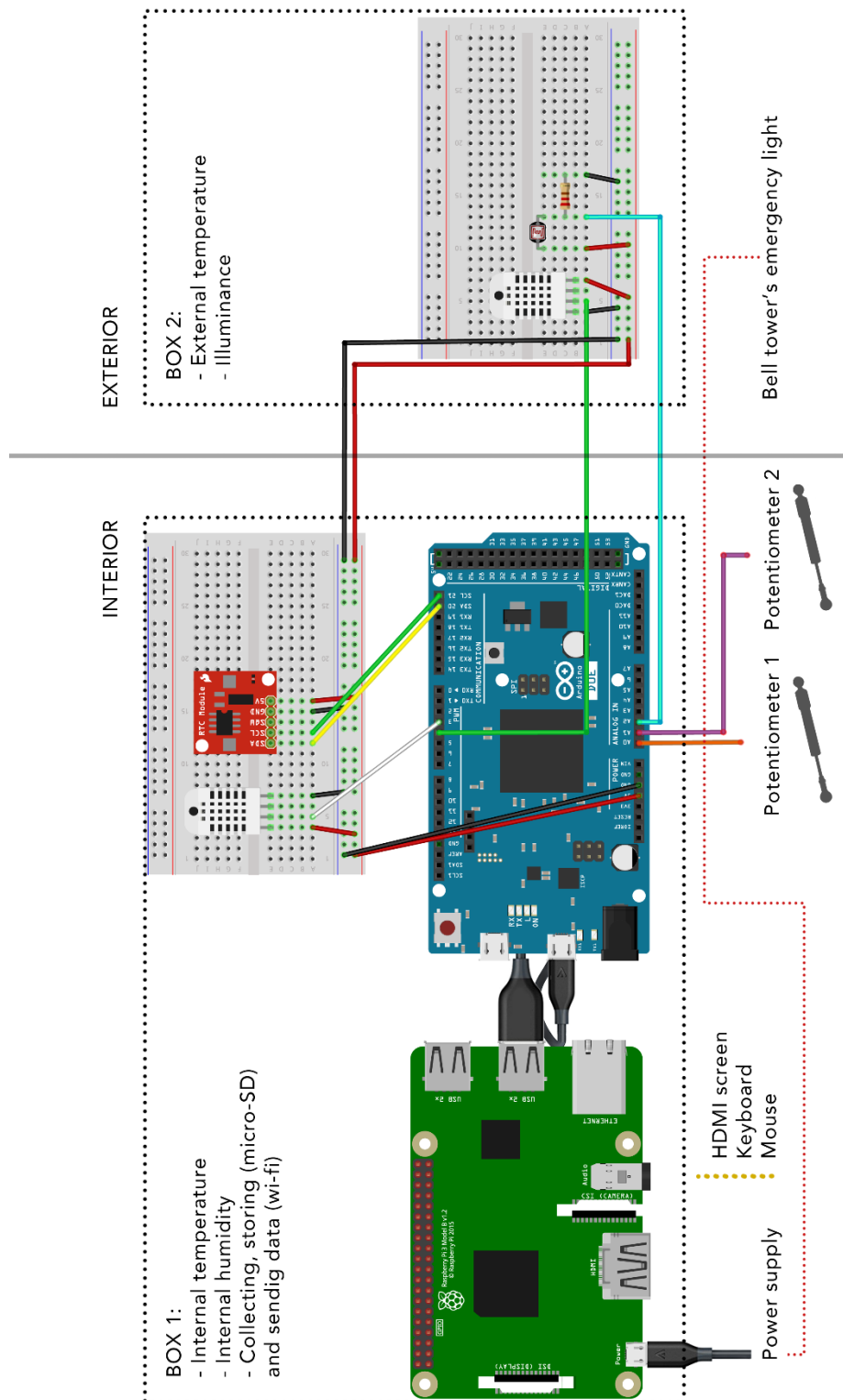


Figure 33: System set-up for Santa Maria del Mar

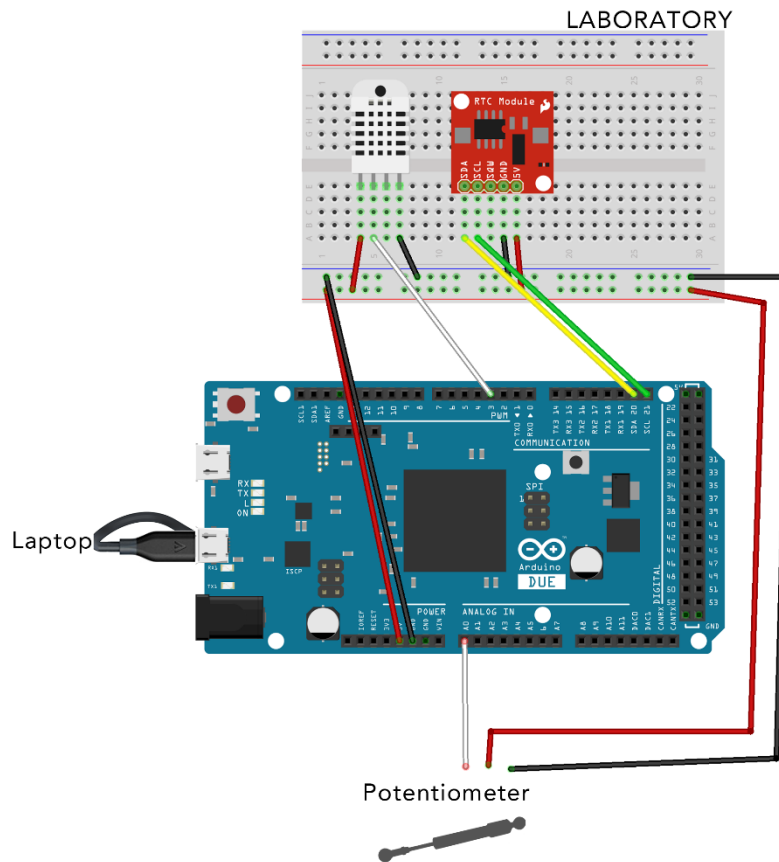


Figure 34: System set-up for laboratory testing

### 4.3 Laboratory test: linear potentiometer

A common mistake in the selection of an ADC is to assume that more resolution always represents a better measurement. The reality is that sensitivity and accuracy have an equal or even greater importance than resolution (DeSantis, 1998). As shown previously, the deployment of a linear potentiometer with a range of 50 mm together with the 10-bit Arduino Yún (or UNO as well) had a resolution of 0,05 mm and an accuracy of  $\pm 0,10$  mm. It demonstrates that resolution is just a part of the problem but is not the main important one at this stage. Moving to a better quality with 12-bit ADC Arduino DUE the system gains a resolution of 0,012 mm and an accuracy of  $\pm 0,027$  mm, while shortening the range to 33mm, moves to 0,008 mm  $\pm 0,018$  mm. From a

theoretical point of view, if all the considerations are corrected until here, the DUE system is able to read a 0,02mm as the smallest difference between two measurements.

#### 4.3.1 System set-up

As shown in Figure 28, the Potentiometer is directly driven by Arduino DUE which is connected to a Laptop through the USB port. The potentiometer is then installed on the Displacement Transducer Calibration Device with one pivot head fixed to the ground and the other one connected to a micrometre through a spring (Fig. 35).

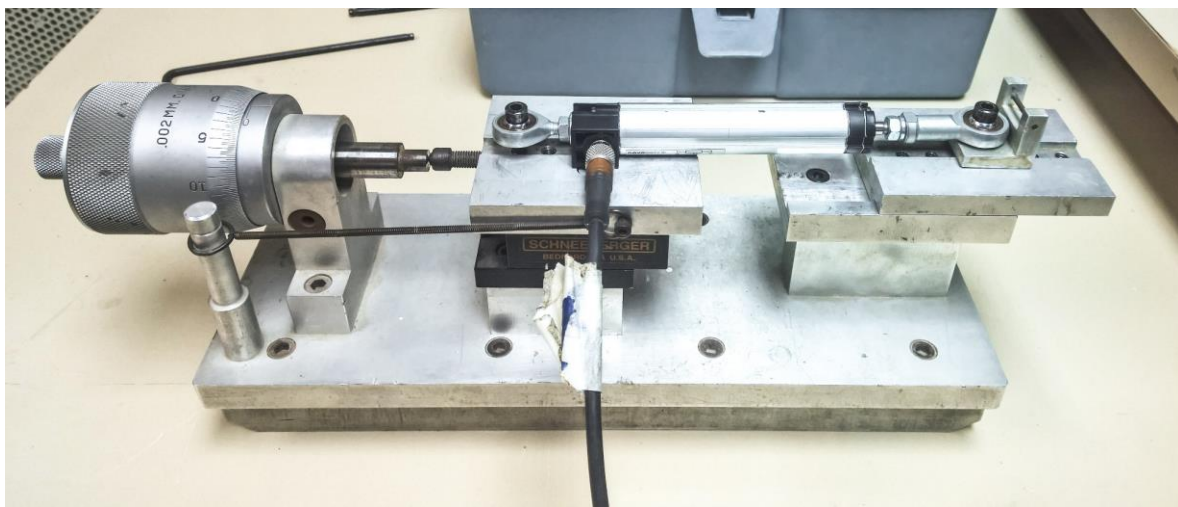


*Figure 35: Potentiometer installed on the Displacement Transducer Calibration Device (resolution 0.002 mm)*

Once installed, the 5V output from Arduino is checked with a multimeter. As it was expected, the signal was very unstable: fluctuating between 4,79V and 4,81V. This issue is very severe when high precision is needed. It can affect the measurement quality producing noise in the data. That means a random fluctuation of the signal. Noise makes difficult recognising a clear value and sometimes can completely cover it or just make the measurement precision worse.

Some preliminary data are recorded on 29 May 2017, to clarify the noise effect on the potentiometer. The Figure 36 represents about 17 minutes of recording at 1 sample per second (S/s) of a stationary position. In other words, the sampling interval (T) is 1 s.

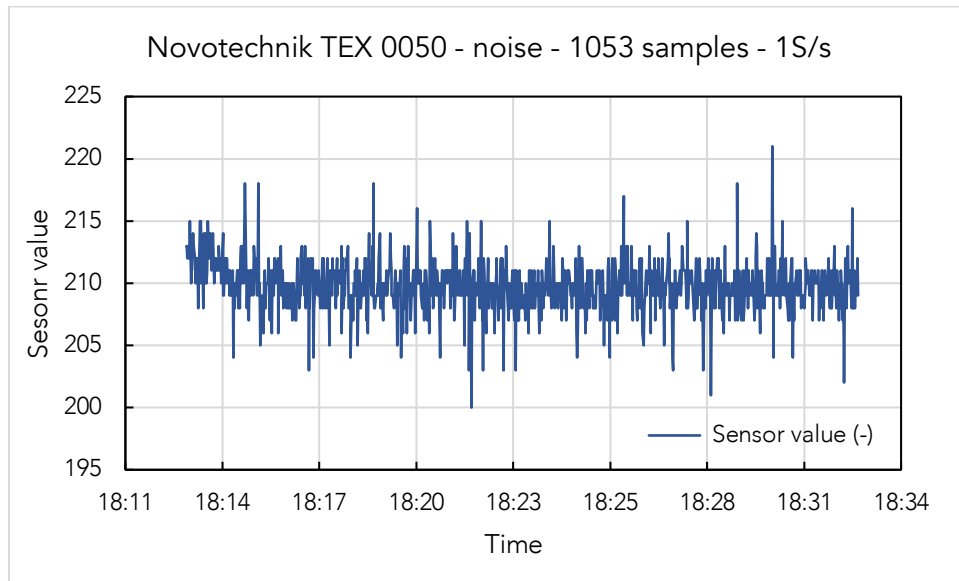


Figure 36: 1053 samples of Novotechnik TEX 0050's noise in a stationary position

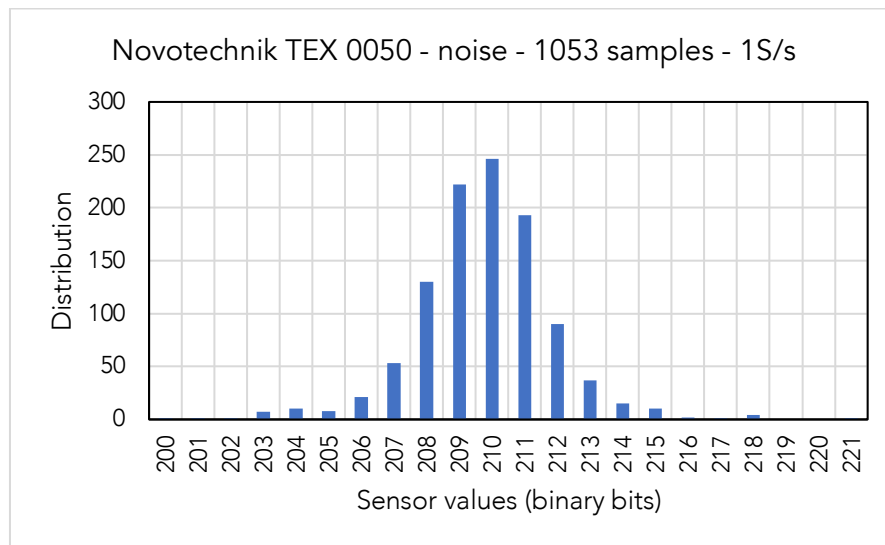


Figure 37: Gaussian distribution of 1053 samples

As shown in Figure 37, a satisfactory normal distribution in the data was obtained. Consequently, the interference showed in Figure 35 is mainly a random noise, so it must be statistically studied. The main ways to represent signal noise are the mean value ( $\bar{x}$ ) and the related standard deviation ( $\sigma$ ) (T. C. Carusone, D. A. Johns, 2012). It is important to point out that this procedure can be applied only on data with a normal distribution.

$$\bar{x}_{noise-1053} = \sum_i^N xi / N = 209,77 \quad (13)$$

$$\sigma_{Noise-1053} = \text{std}(x) = \sqrt{(\sum_i^N (xi - \bar{x})^2 / (N - 1))} = 2,07 \quad (14)$$

Consequently, the value resultant from this brief analysis of the data is 210 ( $\pm 2$ ). It is important to point out that the DUE datasheet gives  $\pm 2,2\text{LBS}$  as lowest precision due to ADC nonlinearity. From this simple consideration, it seems that the real precision of the system is higher than the noise expected from the ADC. In this chapter, no values are converted to millimetres before finding the exact correspondence with experimental results (4.3.3).

In order to understand the dependency of the standard deviation from the number of samples and the sensor level (the physical measure given by the potentiometer), different measurements are reported:

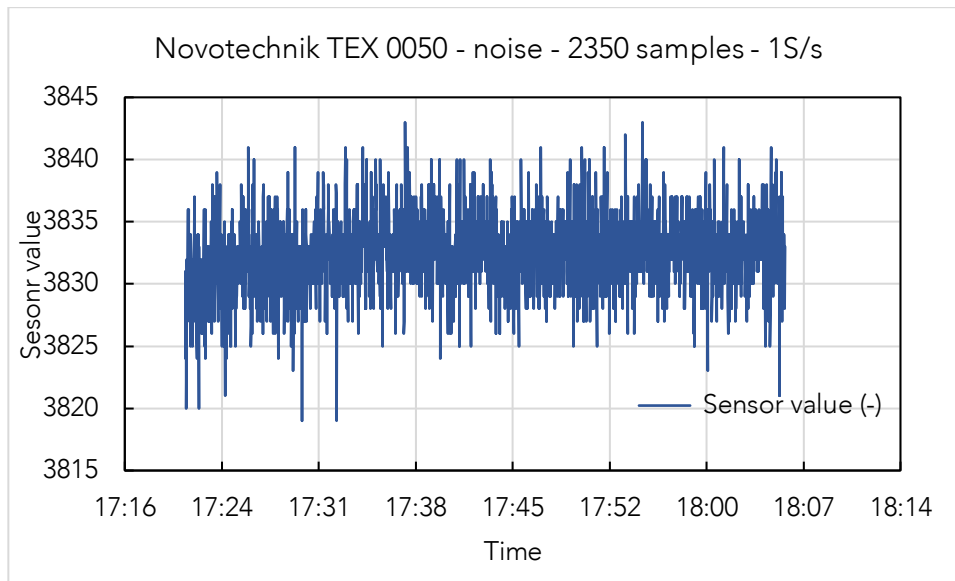


Figure 38: 2350 samples of Novotechnik TEX 0050's noise in a stationary position



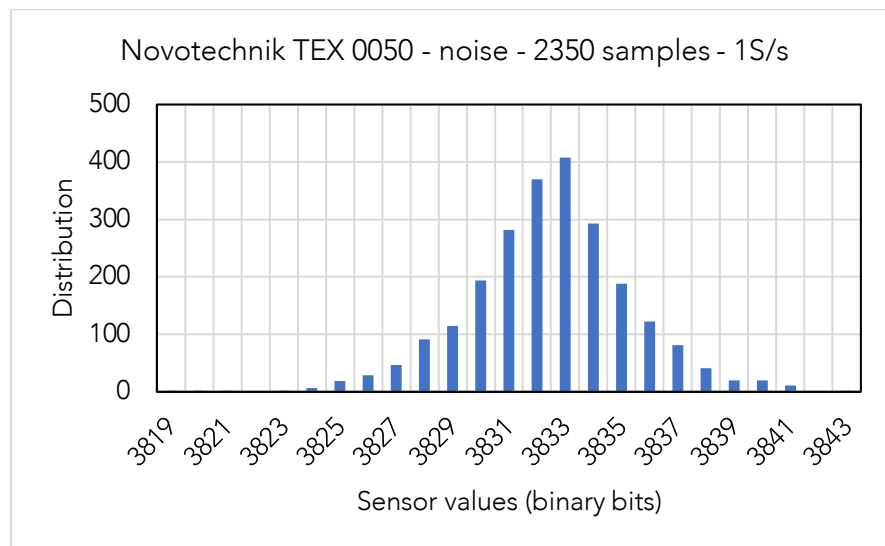


Figure 39: Gaussian distribution of 2350 samples

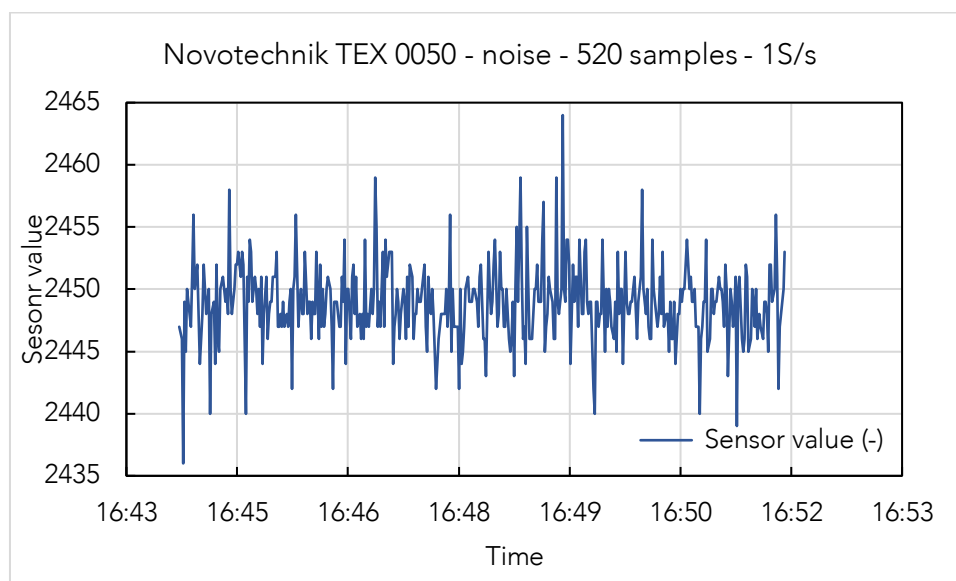


Figure 40: 520 samples of Novotechnik TEX 0050's noise in a stationary position

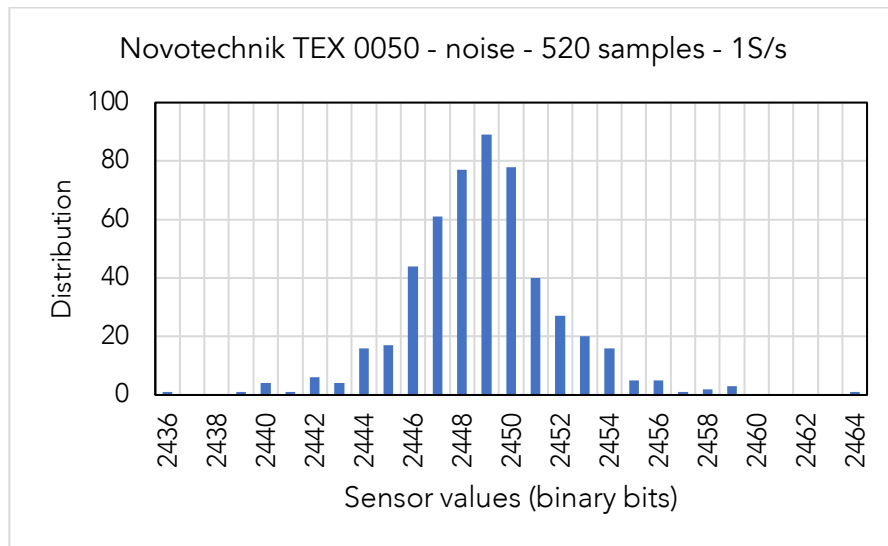


Figure 41: Gaussian distribution of 520 samples

Summarising, the variation of standard deviation doesn't seem correlated with the number of samples or neither with the sensor level as shown in Table 6.

Number of samples	Mean value	Standard deviation	Sample per second
520	2449	3.06	1 S/s
1053	210	2.07	1 S/s
2350	3832	2.91	1 S/s

Table 6: Standard deviation distribution regarding the number of samples

On the other hand, within the same measurement record (i.e. the 2350 samples at 3832 sensor value) it is possible to recognise a very slow rise in the standard deviation if the number of sample is reduced. As shown in Figure 42, the data collected in one record are divided in smaller intervals to understand better the correlation between standard deviation and sample size.

An interesting remark is the signal fluctuation at the beginning of all measurement. Whenever there is a switching event in the microcontroller, a *transient* disturbance appears. The consequence short pulse of current causes a fluctuance in the supply voltage. In case of high-precision measurement the LSB has to be low, and consequently the effects of *transient* disturbance are not negligible. A simple way to avoid this error is cut the affected data in the post-processing.

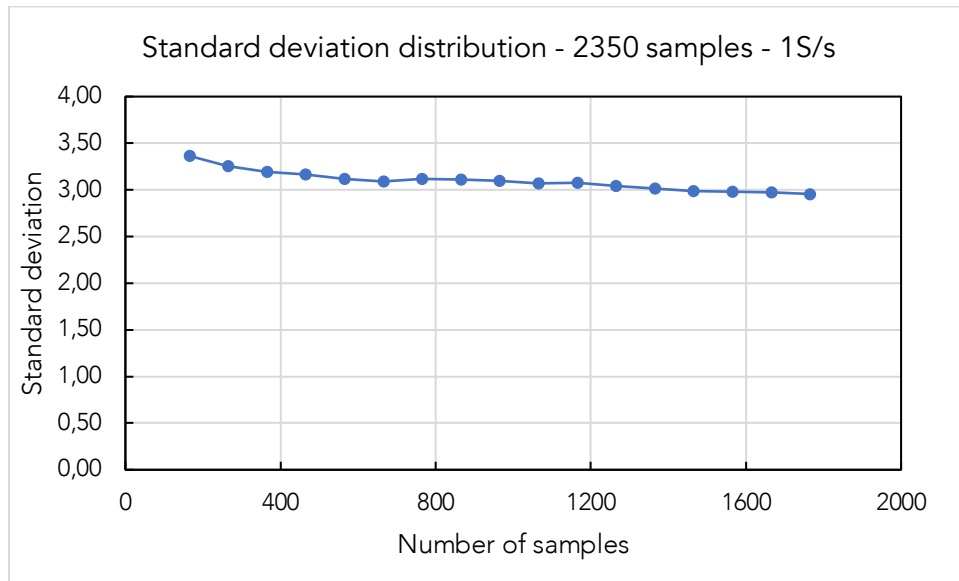


Figure 42: Standard deviation over number of samples of 2350 samples

In conclusion, the effect of the sample size on the standard deviation are not so meaningful from the above considerations. In order to determine the proper number of samples for the calibration of the system, some other considerations on the filtering methods are needed.

#### 4.3.2 Noise filtering

As it is evident from the graphs, some simple statistical techniques to filter out noise are needed. Nevertheless, they can just clean the signal, but any nonlinear effects caused by the ADC or by the sensor remain.

When the sampling distribution is normal, a simple average of the value population helps to improve the resolution. Ideally, averaging reduces the noise by the square root of the sample population. In the case of 4 binary bits of noise, the average of 16 samples should reduce the noise contribution to one:  $\sqrt{16} = 4$ ; and the average  $4 \div 4 = 1$ . The minimum sample size has to be equal to standard deviation raised to the second power. To test this method the 2350 sample record is divided into 146 intervals of 16 samples and then the mean value of each interval is obtained. The peak to peak (PtP) difference of the calculated mean values is equal to 5,94 that is very close to two times the standard deviation (i.e. 5,82). The following graphs show different

dimensions of the interval: it is clear that increasing the interval of averaging the peak to peak difference decreases dramatically.

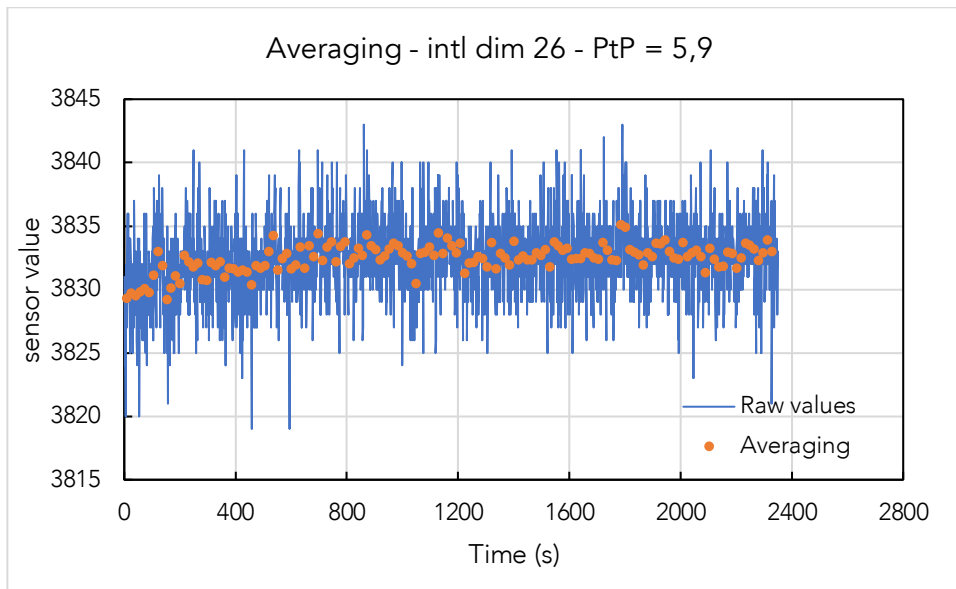


Figure 43: Averaging of the 2350 sample records with an interval on 16 samples

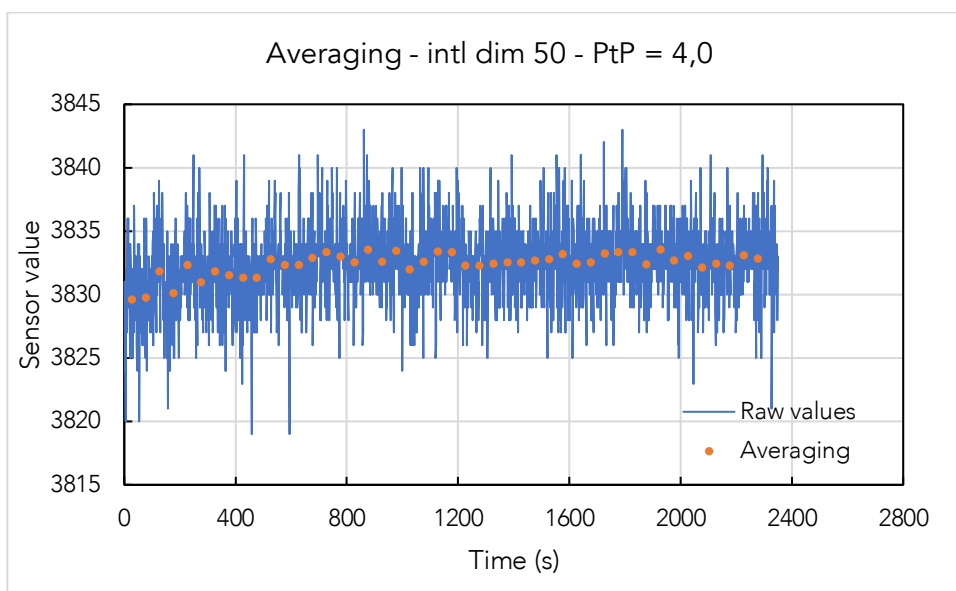


Figure 44: Averaging of the 2350 sample records with an interval on 50 samples

Another very common and easy to use filtering method is the moving average or running average<sup>30</sup>. Instead of dividing the sampled measurements in some interval of a certain dimension, it creates an array of a certain dimension that is updated every time that a new measurement is done. When it reaches the desired dimension, the array starts to give its mean value. Consequently, the signal is composed of the same number of samples.

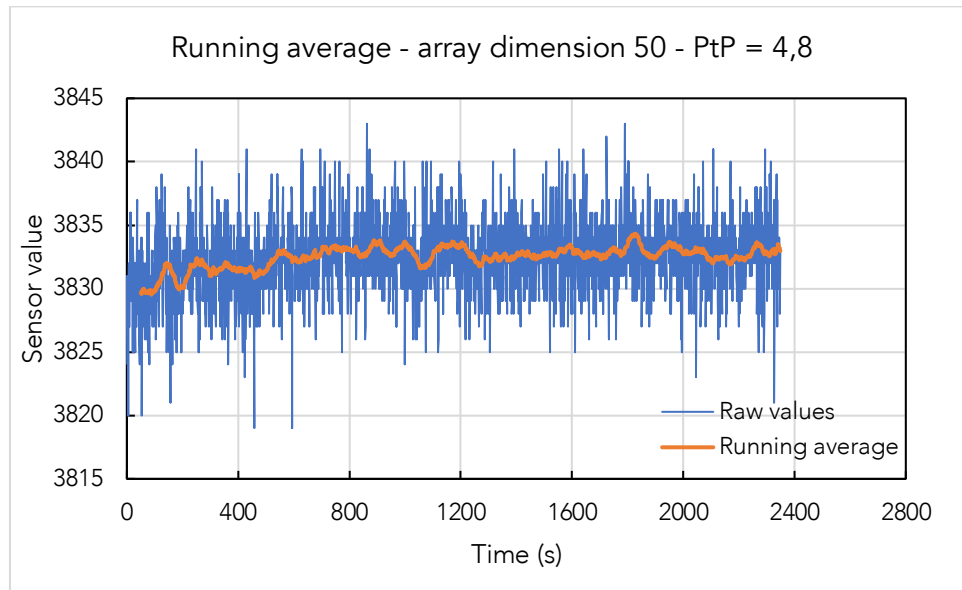


Figure 45: Running average of the 2350 sample records with an array of 50 elements

<sup>30</sup> <http://playground.arduino.cc/Main/RunningAverage>

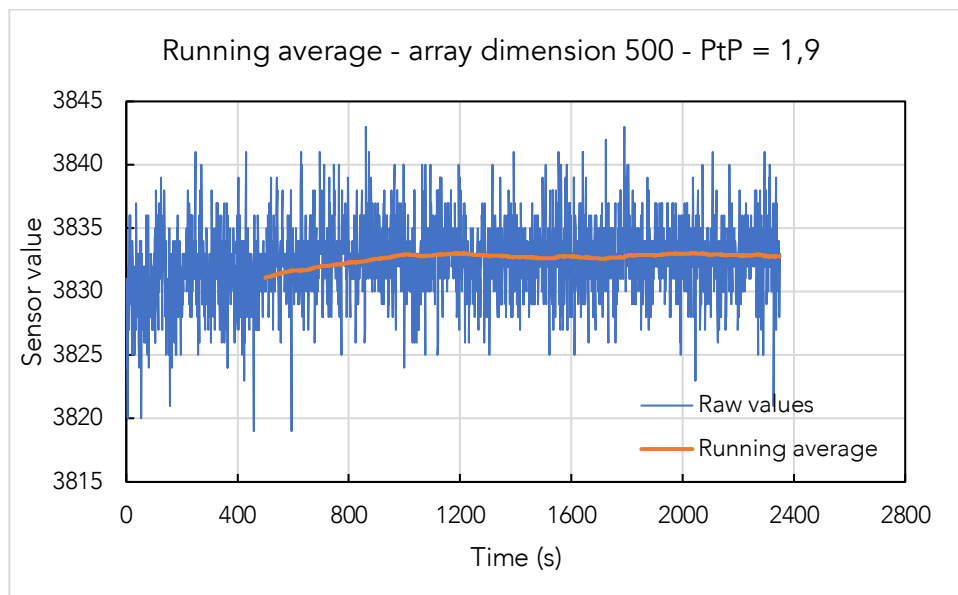


Figure 46: Running average of the 2350 sample records with an array of 500 elements

As it is evident from these graphs, averaging less than 500 samples is not very meaningful. In the following experiences, it is always used a sample size greater than 1000.

#### 4.3.3 Calibration of the Novotechnik TEX 0050

This paragraph has a fundamental importance: evaluating the theoretical considerations developed so far. Particularly challenging is understanding the effects of the interface between Arduino and the linear potentiometer, and the consequences of the unstable output voltage from 5V and 3.3V line. Even more important, there is no exact relationship between the potentiometer's physical displacement and the resulting electrical output. These devices are only relatively precise until an experimental correlation between the output and physical movement is done. This is due to the fact that the exact physical length of the resistor element cannot be controlled with an absolute value during manufacture. In the technical specification is reported: body length  $\pm 2\text{mm}$ . The experiment took place the 16<sup>th</sup> of June 2017. It is divided into 19 steps, each time a certain number of samples are recorded and analysed (Rec). Between one step and the progressive one, a certain displacement is applied with the Displacement Transducer Calibration Device. In the next chart, the data acquisition and data post-processing workflows are shown:

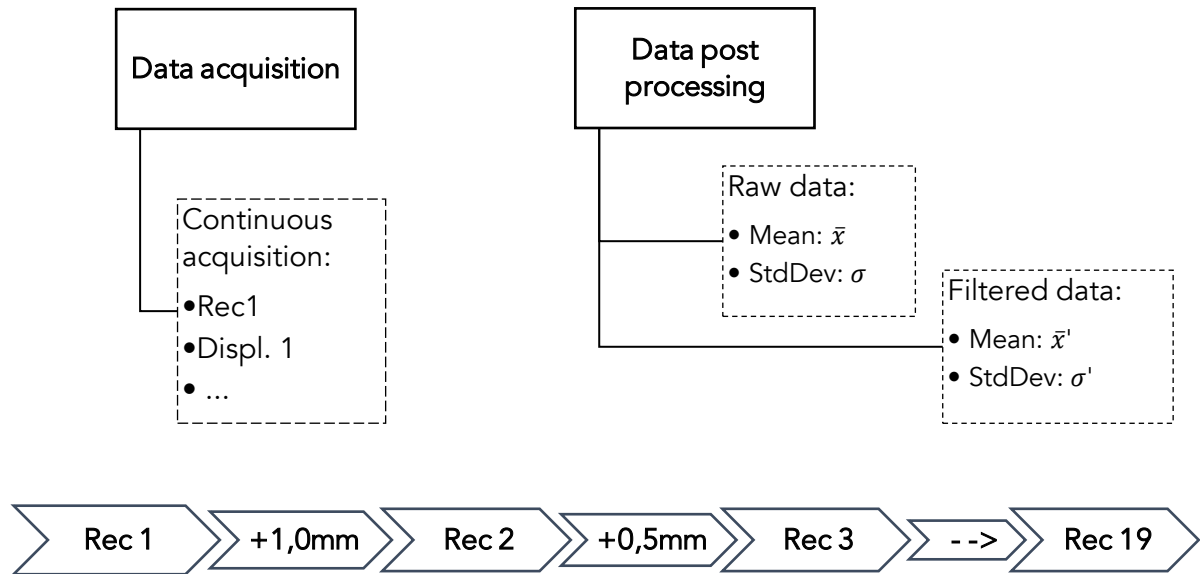


Figure 47: Data acquisition and data processing workflow at Camins Maker Lab 16/07/2017

Figure 48 shows the entire recordings through the experiment. Especially after 17:45 the steps are clearer since the applied displacement is bigger. Furthermore, in the beginning there was a very noisy signal and for this reason the first step was not considered in the analysis (see Table 6).

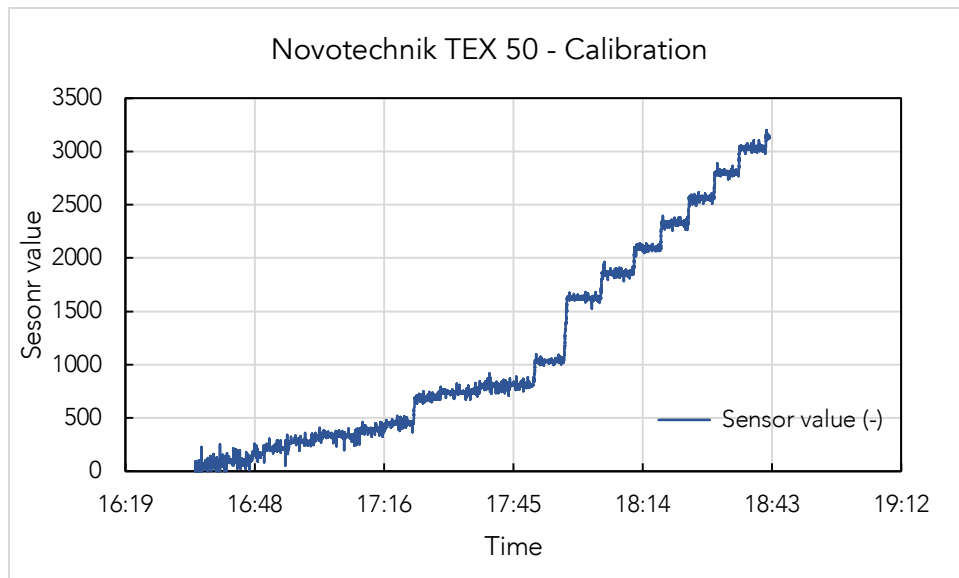


Figure 48: Complete recordings of calibration experiment at Camins Maker Lab 16/07/2017

It is important to point out that for the first time another disturbance was noticed: *voltage spikes*. The voltage spike is a sudden and very short-in-time increase of tension.

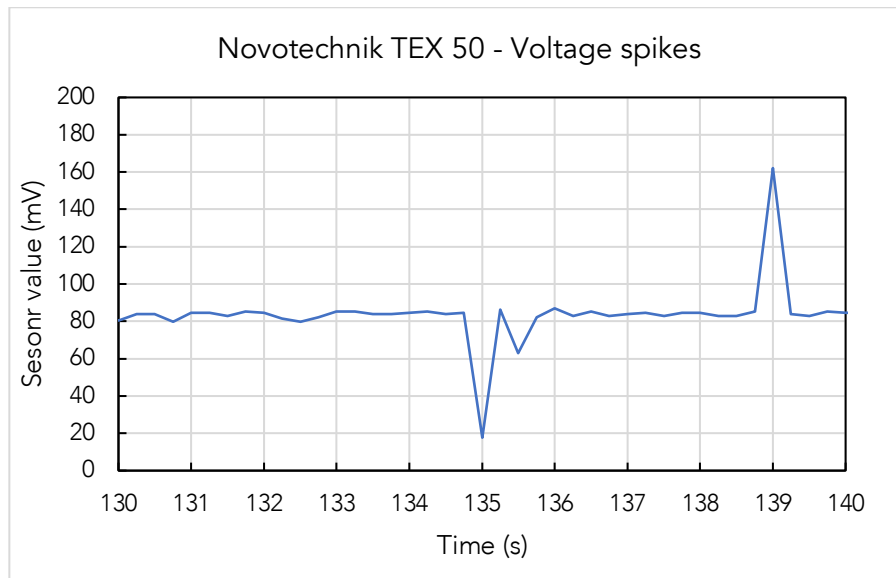


Figure 49: Voltage spikes on collected data

Several issues can cause voltage spikes, from loss of data to interaction with a nearby magnetic field<sup>31</sup> but unfortunately, the most probable cause in this application is damaged equipment.

From the first day, a high pitch noise was detected in this model of Arduino DUE. Conversely, it wasn't a serious issue in the beginning. After some weeks, it started to be more frequent, and in case it was present after the sketch upload, the voltage distribution has a completely no sense. This problem was detected by other users of this board<sup>32</sup> and probably is caused by a defect in the decoupling capacitor: the only way to completely solve it is board substitution.

As it is evident from the graph in Figure 49, the peaks created by the spikes have to be deleted. The LSB is 0,81 mV, and the greater spike increases the voltage level about 80 mV (99 in binary bits). A simple technique is to calculate the mean value and the standard deviation of each step and then replots the data cutting all values greater than  $\pm$  two times the standard deviation.

<sup>31</sup> <http://study.com/academy/lesson/voltage-spike-definition-causes-protection.html>

<sup>32</sup> [https://www.reddit.com/r/arduino/comments/5q57pw/high\\_pitch\\_noise\\_on\\_new\\_arduino\\_due/](https://www.reddit.com/r/arduino/comments/5q57pw/high_pitch_noise_on_new_arduino_due/)



Summarising, in data acquisition and post processing some of the problems detected so far are solved as follow:

- Switching *transient* disturbance -> continuous acquisition of data;
- Random spikes -> cut the band of values greater than  $\pm 2$  times the raw data standard deviation ( $2 \cdot \sigma_i$ );
- Random noise -> averaging the filtered sample recordings ( $\overline{x_i'}$ ).

$\overline{x_i}$  and  $\overline{x_i'}$  are the mean values of the i-th step, and  $\sigma_i$  and  $\sigma_i'$  are the standard deviations of the i-th step, respectively, for the raw and of the filtered data.  $d_i$  are the applied displacement each step. From this post processed data, the difference between each step ( $\Delta_i$ ), the i-th calibration factor ( $cf_i$ ) and the weighted average of the calibration factor ( $\overline{cf}$ ) are calculated as follow:

$$\Delta_i = x_i - x_{i-1} \quad (-) \quad (15)$$

$$cf_i = d_i / \Delta_i \quad (mm) \quad (16)$$

$$\overline{cf} = \frac{\sum(cf_i \cdot d_i)}{\sum d_i} (mm) = 0.00853 (mm) \quad (17)$$

Step $i$	2	3	4	5	6	7	8	9	10
$n^\circ$	1301	1300	1300	1300	1300	1301	1299	1301	1299
$\bar{x}_i$	103.5	217.76	277.26	333.59	391.40	452.15	685.59	740.31	799.52
$\sigma_i$	9.87	8.18	6.24	6.60	7.29	7.86	6.94	7.50	8.24
$\bar{x}'_i$	103.5	217.71	277.09	333.48	391.42	451.35	685.38	740.19	799.39
$\sigma'_i$	2.85	2.52	2.49	2.54	2.74	3.19	3.85	3.56	3.56
$\Delta_i$		114.22	59.38	56.39	57.94	59.93	234.04	54.81	59.19
$cf_i$		0.0088	0.0084	0.0089	0.0086	0.0083	0.0085	0.0091	0.0084
$d_i$		1.00	0.50	0.50	0.50	0.50	2.00	0.50	0.50
$\bar{cf} \cdot \Delta_i$		0.974	0.506	0.481	0.494	0.511	1.995	0.467	0.505
$\bar{cf} \cdot \Delta_i - d_i$		0.03	-0.01	0.02	0.01	-0.01	0.00	0.03	0.00
Step $i$	11	12	13	14	15	16	17	18	19
$n^\circ$	1301	1300	1301	1301	1301	1301	1299	1300	1301
$\bar{x}_i$	809.5	1033.96	1623.49	1859.63	2092.90	2329.45	2565.08	2800.13	3036.70
$\sigma_i$	7.13	5.26	5.81	7.89	6.73	7.32	7.36	7.27	7.10
$\bar{x}'_i$	809.5	1033.95	1623.32	1859.66	2092.91	2329.46	2565.32	2800.11	3036.79
$\sigma'_i$	3.10	3.22	3.85	4.34	4.36	4.63	4.58	4.72	4.71
$\Delta_i$	10.12	224.44	589.37	236.33	233.26	236.55	235.86	234.79	236.68
$cf_i$	0.0099	0.0085	0.0085	0.0085	0.0086	0.0085	0.0085	0.0085	0.0085
$d_i$	0.10	1.90	5.00	2.00	2.00	2.00	2.00	2.00	2.00
$\bar{cf} \cdot \Delta_i$	0.086	1.913	5.025	2.015	1.989	2.017	2.011	2.002	2.018
$\bar{cf} \cdot \Delta_i - d_i$	0.01	-0.01	-0.02	-0.01	0.01	-0.02	-0.01	0.00	-0.02

Table 7: Calibration of the Novotechnik TEX 0050

#### 4.3.4 Final remarks

The minimum displacement measured is 0,10 mm and the max/min differences between the physical displacement imposed with the micrometre ( $d_i$ ) and the one measured ( $\overline{cf} \cdot \Delta_i$ ) are -0,02 mm and +0,03 mm.

That means the system has a resolution of 0,10mm, an accuracy of  $\pm 0,03$ mm and LSB expressed as a distance of 0.00853 mm (i.e. the average calibration factor). The expected minimum difference in two consecutive readings was 0,02mm, five times less than what was obtained with this experiment. As mentioned at the beginning of the paragraph, the voltage spikes are a strong indication of some unsolvable problems from a statistical processing of data. Looking at the standard deviation of the raw data recorded the 29<sup>th</sup> of March and the 16<sup>th</sup> of June, there is a severe increase in comparable voltage/sensor level:

Day	Sensor level	StdDev (Raw data)	StdDev (Filtered data)
29/05	210	2,07	-
	2149	3,06	-
16/06	218	8,18	2,52
	2093	6,73	4,36

Table 8: Variation in standard deviation between the 29/05 and the 16/06

A method to come back to similar data distribution is filtering. The procedure explained in the previous paragraph, allows to delete the voltage spikes but not random fluctuation in the signal, probably created by the ADC. Furthermore, there is almost a proportional increase in the corrected standard deviation ( $\sigma_i'$ ) compared with voltage/signal increase. More the signal gets closer to the 4095 binary bits, more the noise arises in the output signal.

In Figure 50, 51 and 52, the effects of these interferences very are clear.

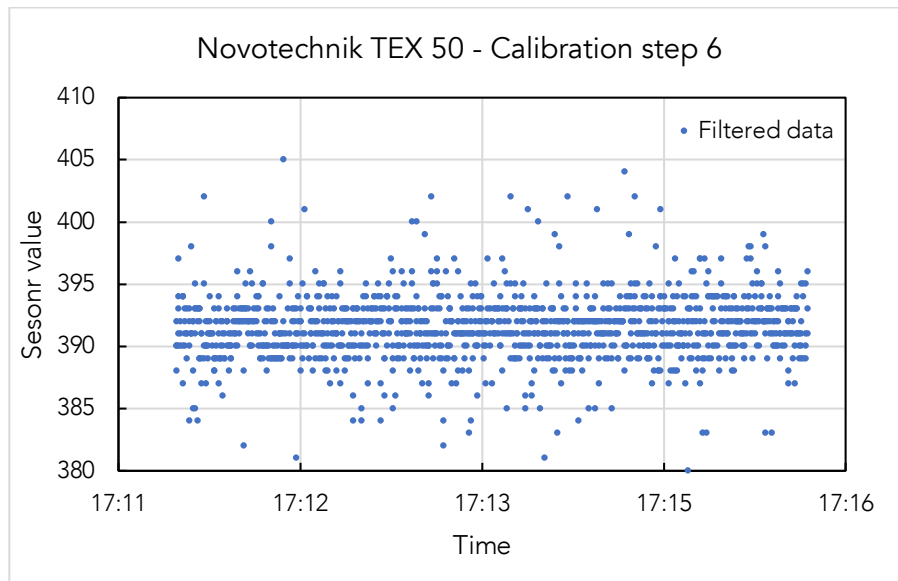


Figure 50: Filtered data without significant fluctuation ( $\text{StdDev}=2,74$ )

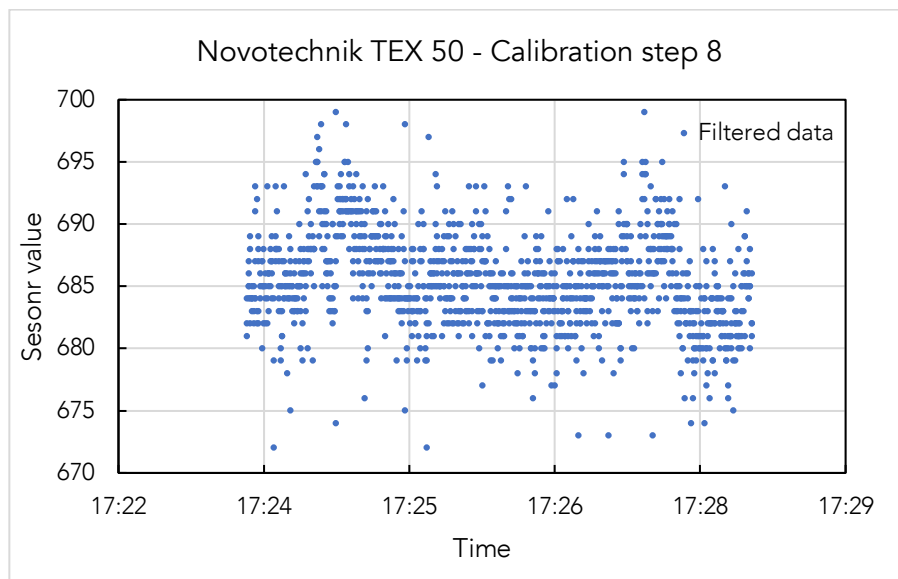


Figure 51: Filtered data with significant fluctuation ( $\text{StdDev}=3,85$ )

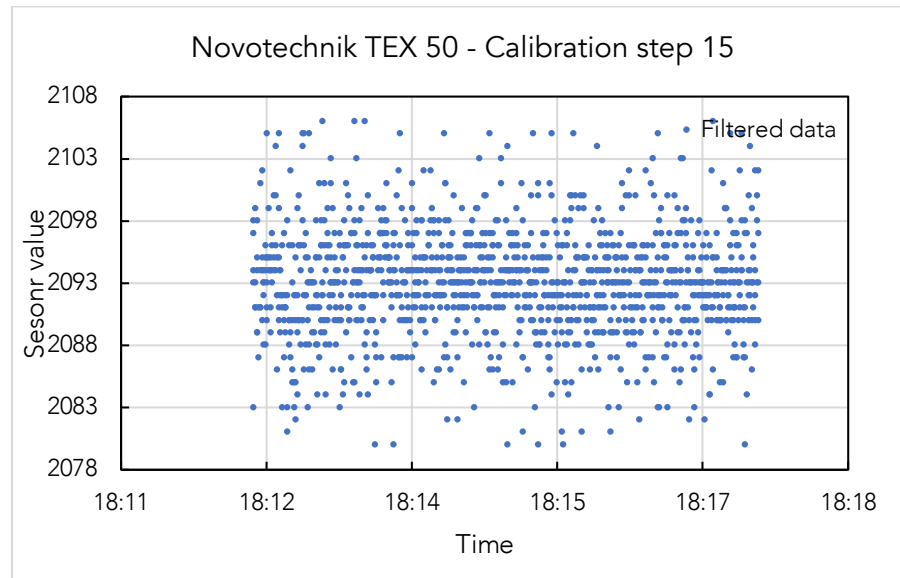


Figure 52: Filtered data with a significant increase of noise (StdDev=4,36)

In light of what we have shown up to this point, to obtain a reliable and stable system on the long-term, the entire layout has to be reconsidered and redesigned. Especially according to the following issues:

- Noise in sensor's power supply
- Noise in sensor's signal
- More accurate ADC with 12-bit or greater resolution

#### 4.4 Further improvements: strategies for building a reliable system

As it is evident from the last paragraph, to meet the main aim of this research further improvements are needed. Through the deployment of the linear potentiometer, instead of the LVDT, the system's cost decreased dramatically, but the reliability is still a problem. Especially the noise level detected during the calibration process is not admissible. Consequently, the specific objectives of the following paragraph are:

- Deployment of an external linear stable voltage supply
- Clean the sensor's output
- Select another ADC with a real 12-bit resolution or even higher

Due to unsolved signal problems, focusing on the voltage supply, ADC quality and sensor structure is now fundamental. Previously, the analysis of Arduino's ADC and noise filtering techniques while taking a lot of time, did not give the expected results.

##### 4.4.1 Introduction: a new block diagram for the linear potentiometer

According to Mancini (Mancini, 2002), the diagram shown in the figure is the typical transducer measurement system. A power supply and eventually a voltage reference are the energy source of the system. The bias or excitation circuit feed the transducers with the proper tension. The transducer converts a physical magnitude (the called input variable) into an electrical signal. Finally, the ADC sends the output data to a digital microcontroller.

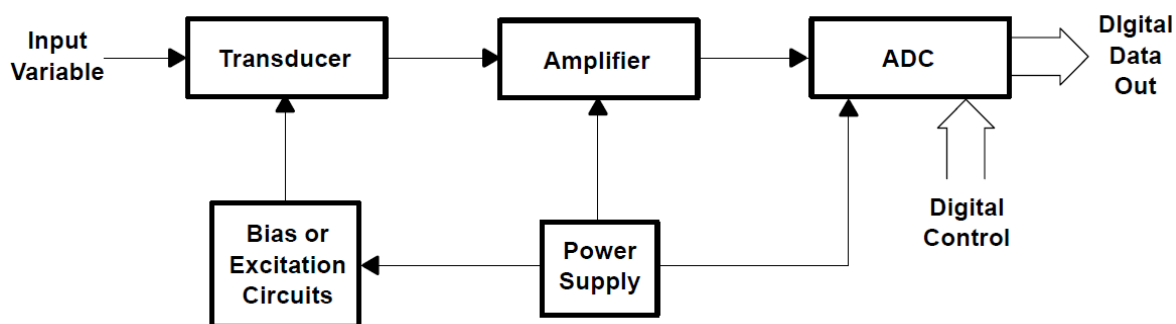


Figure 53: Typical Block Diagram of a Transducer Measurement System

#### 4.4.2 Precision voltage reference

As stated by Miller (Miller and Moore, 1999), the system accuracy of a data conversion system is very much dependent on the accuracy of the voltage established by an internal or external direct current (DC) voltage reference.

In analog-to-digital converter (ADC) the analog input signal together with the DC reference voltage is used to produce the digitalized output. Any error in the reference voltage is directly reflected in the output signal. In the case of Arduino DUE, the analog-to-digital converter (ADC) has an internal 3.3V reference quite unstable. Before discussing the change of the ADC is clear that an external precision voltage reference is required. As listed by Miller (Miller and Moore, 1999), relevant parameters for the selection of a DAS reference voltage are: initial error, output voltage temperature coefficient (TC), thermal hysteresis, noise, and long-term stability. To have a direct correlation with the 12-bit ADC (or its multiple), a reference voltage of 4.096V is recommended. Examples of 4.096 reference voltage are: LM4040 by Texas Instrument or MAX6220 by Maxim Integrated.

A low noise linear power source of 5V has to be used. It is important to point out that the voltage reference has to be the same for the external ADC and the potentiometer.

#### 4.4.3 The Novotechnik linear potentiometer

Novotechnik is a German company based in Ostfildern that introduced the potentiometer into the mechanical engineering sector in the 50s<sup>33</sup>. The linear potentiometer deployed in this research has a simple structure. It provides a radiometric output, and that means an output signal which changes proportionally with the input voltage. In order to reach the desired resolution and accuracy some rules have to be respected:

- The output signal is free-of-noise only if the voltage applied is free-of-noise.
- This linear potentiometer is a purely analog device and powers it on a digital device can increase the input noise dramatically.
- And the main important: no current has to flow in the wiper.

---

<sup>33</sup> <http://www.novotechnik.com>

Regarding the last point, it is stated in the technical specification that less than  $1\mu\text{A}$  is a necessary condition for the right sensor's performance. Indeed, it directly affects signal linearity due to localised heating of the resistive element.

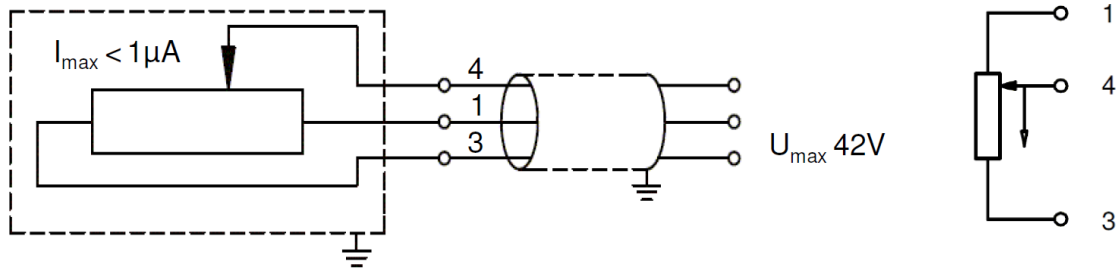


Figure 54: Shown configuration for extended position of the actuating rod (left) and schematic view of wiring (right): 1 power, 4 signal and 3 ground

Consequently, the transducer has to be powered with a low noise voltage reference and then connected with a voltage follower. This component is an op-amp circuit with a gain of tension equal to one, that means an op-amp with no signal amplification. Indeed, its purpose is just to avoid current flow. Since op-amp circuits have a very high input impedance (i.e. high electrical resistance), a minimal amount of current can flow according to the ohm's law (Mancini, 2002).

#### 4.4.4 External ADC

As it is widely explained in paragraph 4.1.2, a crucial importance is deploying an accurate ADC with a clean power supply and a clear signal from the transducer. Another op-amp voltage follower is used as an interface between the ADC and the 4.096 voltage reference. Some of the converters that can be deployed are the ADS1115 16-Bit by Adafruit or the MCP3208 12-bit by Microchip Technology.

#### 4.4.5 Final remarks

In conclusion, it is clear that further improvements are needed before a low-cost solution can be compared to a professional one. The block diagram proposed below has already solved all the problems that arose during this 3-month research. On the other hand, as demonstrated during this thesis, is hard to ensure reliability without laboratory experience.



## 5 DEPLOYMENT ON A CULTURAL HERITAGE BUILDING: SANTA MARIA DEL MAR

This chapter focuses on the design of a continuous static monitoring system for monumental structures: the case of Santa Maria del Mar church in Barcelona.

### 5.1 Introduction on the problem

Santa Maria del Mar is one of the most interesting examples of Catalan Gothic architecture ever built and one of the main touristic and spiritual attractions of the capital of Catalonia. Built during the 14<sup>th</sup> century, in its long history, the Church suffered different calamities that caused severe damages: fires (1379 and 1936), earthquakes (1373 and 1428) and bombardments (1714 and 1936-1939) (González et al., 2008). Since it is intrinsically fragile, it is even more important to monitor and study the evolution of active damage patterns.



*Figure 55: Santa Maria del Mar: interior (left) nave and main façade (right)*

After the most recent restoration of the main façade a couple of years ago, a closed crack appeared again showing an active phenomenon. It is located in the proximity of the south-west belfry while a second crack appeared on the lateral façade approximately on the same height. In this context, the UPC professors Luca Pelà and Rolando Chacón proposed to the parish (i.e.

Parròquia) to install a low-cost monitoring system to study and control the evolution of the damage pattern.

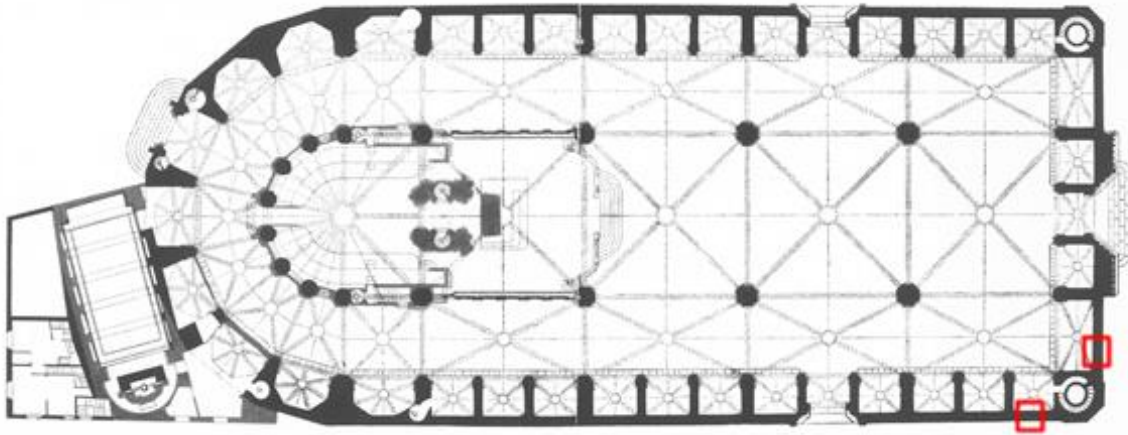


Figure 56: Plan of the church and the position of the two cracks

## 5.2 Historical information

When the first Christians arrived in the Roman colony of Barcino, the ancient name of Barcelona, a small community was founded near the sea, just outside the city walls. In this area, there was a Christian necropolis, probably located on the rests of a Roman theatre (Carbonell, 2011) where Saint Eulalia martyr was buried in 303 A.D., under the empire of Diocletian (284-305 A.D.). This site might have been the place where a chapel was first built and named "Santa Maria de Les Arenes". By the end of the seventh century, the structure was already known as "Santa Maria del Mar"<sup>34</sup>.

During the 13th century the city grew, and the neighbourhood called "La Ribera" became richer. The wealthy merchants and minor nobility that had built their houses there started to demand a church of more impressive dimensions and beauty. Church authorities supported the initiative, merchants donated money, and King Pere III gave his permission to extract stone from the quarry to build the new church<sup>35</sup>. The cornerstone of the present church was laid on 25 March 1329, as the two inscriptions on each side of the door on Santa Maria Street testify. The project was

<sup>34</sup> <http://www.santamariadelmarbarcelona.org/history>

<sup>35</sup> <http://www.santamariadelmarbarcelona.org/history>

followed by the architects Berenguer de Montagut and Ramon Despuig, two of the main representatives of the Spanish Gothic. The last circular Keystone, close to the main door, represents Barcelona's coat of arms and was placed on 3 November 1383. On 15 August 1384, the bishop of the city finally consecrated the church, although the bell towers (1496 and 1902) and the old rose window were left to build (Martínez Gil, 2017).

Over the years some calamities occurred: on 26 December 1378, a fire destroyed part of the sacristy, the choir, the organs and some altars. Due to this fire, in 1379 extensive restorations were done (González et al., 2008). The church was damaged again the 2 February 1428, when an earthquake caused the collapse of the old rose window and some damages on the façade. Then, on the night of 19 July 1336, the civil war caused a huge fire that completely destroyed the baroque altar and all the images and the historical archive of the church.



*Figure 57: Before (left) and after (right) the fire of 1936 (Martínez Gil, 2017)*

### 5.3 General description of the building

Despite the damages, Santa Maria del Mar remains one of the more beautiful examples of religious architecture in Catalan Gothic. The pointed arches, the rib vaults with their nerves converging to the vault's key and the very thin pillars are clear features of Gothic that can be

distinguished from the massive structures of the Romanesque. To the habitual characteristics of Gothic architecture, some peculiarities of Gothic-Catalan have to be added, such as the equalisation of the heights of the ships, so that the interior space is larger and gives a feeling of a spacious room (Martínez Gil, 2017).

The church is composed of three naves, a semi-circular apse with ambulatory and nine radial chapels: these result from the space between the end of the lateral naves and the end of the buttresses, as used in the Catalan Gothic style (Murcia, 2008). The naves are divided into four square sections, all sustained by octagonal columns and covered by cross vaults; each cross-section also has three lateral chapels (16 metres high). The columns are 13 metres high and are separated by 13 metres from each other.

The building is almost 85 metres long, 35.30 metres wide, and has a maximum height of 34 metres from the ground to the roof. On the corners of the southern façade, there are two towers (47 metres high the western one and 46 metres high the eastern one), both integrated into the lower part of the perimeter of the façades. There are four entrances: the main one on the main façade brings to the central nave, and has a big portal (12 metres high) decorated with sculptures; the other entrances (one at the head, and two to the lateral naves at the lateral façades) are similar but smaller and simpler. The main façade has two longitudinal buttresses, and a 9-metre diameter rose window in the centre. The cover of the lateral chapels created a terrace level, that is used for the circulation of people. There are four buttresses at each lateral side of the church, two in the main façade and six at the head, all 14 metres high but with different wide (from 1.50 to 1.38 metres).

## 5.4 Monitoring proposals

As mentioned at the beginning of the chapter, the damages object of this study are two cracks located in the proximity of the south-west bell-tower. According to Martínez (Martínez Gil, 2017), these damages are the results of a differential settlement of the tower in respect of the rest of the church and they could be easily connected to the seasonal movement of the groundwater. Very likely this is the reason for their activity: during a recent restoration, they were closed and now are clearly visible.

The following proposal was realised by prof. Luca Pelà, arch. Jordi Portal and prof. Rolando Chacón with the support of Saray Martínez Gil, to present the novel monitoring system to the parish of Santa Maria del Mar. It consists in the development of a low-cost monitoring system for the digitalization of the behaviour of the cracks in Figure 56. In doing so, the real causes of the phenomenon can be enquired, and more conscious action can be taken. The whole intervention is guided by the principle of minimum intervention and minimum visual impact. The data collected from this system are sent through wi-fi connection and then storage and analysed at UPC. The system is composed of the following sensors:

- Displacement sensor (Novotechnik Linear Potentiometer): to capture the opening-closing cycles of the fissure.
- Sensors of temperature and humidity (Adafruit DHT22): sensors will be necessary to the interior and exterior since the cyclical movements of the cracks are related to the environmental variables.
- Light sensors (LDR): with the objective of being able to measure the sunlight to the outside and to establish a relation between the movements of the crack with the cycles of day and night.

The Data Acquisition System is composed by an Arduino DUE while the Data Transmission System is constituted by the microcomputer Raspberry Pi 3. Therefore, the data collected are sent to a digital cloud at UPC called SmartLab device enabling the real-time control and analysis. In order to take the system less visible as possible and minimise the visual impact of DAS and DTS, 3-D printing technologies are used to create a proper case, aesthetically compatible with the Cultural Heritage.

## 5.5 Design of the system set-up

The requirement for the correct set-up of the systems are:

- Access to the wi-fi network of the Church by the Raspberry Pi.
- Continuous current to supply the Raspberry Pi and the equipment necessary during the set-up of the system, namely the LCD screen.





*Figure 58: Monitoring proposal*

After a meeting with the architects that represented the parish, the following solution was developed:

- The system will be supplied by the emergency continuous current present in the bell-tower;
- A tripolar cable will pass from the electrical box in the tower through a small hole in the masonry wall between the joints and then will feed the DAS and the DTS;
- DTS, DAS and temperature/humidity sensor will be enclosed in a case just above a small altar of the Virgin Mary, few meters far from the crack on the main facade;
- From this point, all the cables will start and connect the different sensors.
- The external temperature/humidity and light sensors will be set-up in the easy-accessible window in the bell-tower.

In conclusion, Figure 58 represent the selected monitoring proposal: red is the interior temperature and humidity, DAS and DTS, yellow refers to Potentiometer 1, green refers to Potentiometer 2 and purple to the power cable and the external temperature within the bell-tower.





## 6 CONCLUSIONS

### 6.1 Summary

The present research is a contribution to the development of a low-cost, open-source, reliable and accurate system for the structural monitoring of monumental buildings and more broadly of Cultural Heritage. Particularly, it focuses on the determination of the real system resolution. In summary, the most important steps faced during the thesis were:

- In the beginning, a review of available procedure and instruments for SHM was completed. Particularly, an analysis of displacement sensors was necessary to understand their electrical and mechanical operation.
- At the same time, the state of the art of open-source hardware was illustrated. Since it is a rapidly evolving field, it is fundamentally a continuous study: a series of microcontrollers, microcomputers, environmental sensors and communication modules were enquired.
- An accurate analysis of past research experiences at UPC was completed. Particularly, the first approach to low-cost structural monitoring by Basto (Basto, 2015) and a further application focused on Cultural Heritage application by Martinez (Martínez Gil, 2017). In both cases, very promising results were shown, and some limitations related to noisy signal and ADC resolution were experienced.
- An improved system based mainly on Basto and Martinez conclusions was set up to overcome the mentioned limitations. It is composed of an Arduino DUE as DAS, a Raspberry Pi 3 and the SmartLab device as DTS, a Novotechnik linear potentiometer as displacement control sensor and an Adafruit DHT22 as temperature and humidity sensors. The theoretically calculated resolution, based on Arduino ADC characteristic and nonlinear effects is equal to 0,01mm ( $\pm 0,02$ mm).
- Testing was then necessary to understand the effects of noise on the signal resolution. Through a Displacement Transducer Calibration Device, a known displacement was induced and the data coming from the potentiometer recorded.
- The collected data were highly affected by noise. For this reason, a statistical analysis was necessary. Firstly, the raw data were analysed and the voltage spikes filtered out

neglecting values greater than two times the standard deviation. Secondly, from the filtered data the calibration factor was determined. Finally, the resolution of the tested system was equal to 0,1mm with an accuracy of  $\pm 0,03$ .

- The final step was the design of the static monitoring system for Santa Maria del Mar. According to the architects in charge, the best solution was selected and will be probably installed in September. The necessary monitoring period will be two years: the first one to understand and filter out the environmental effects, and the second one to clearly analyse the phenomenon.

## 6.2 Specific conclusions

In the light of the results obtained and observations made during the present research, it is possible to draw the following conclusions:

- The easiest, controllable and convenient way to connect a microcontroller to wi-fi is through the microcomputer Raspberry Pi.
- The single microcontroller with a 12-bit ADC integrated into the board and price lower than 50€ is Arduino DUE.
- The most suitable displacement sensors for low-cost Do It Yourself application is the Linear Potentiometer.
- Different low-cost temperature sensors were tested: the most stable and accurate one for high-precision application is the Adafruit DHT22.
- The minimum displacement measured during the calibration test was 0,10mm, and max/min differences between the physical displacement imposed with the micrometre and the one measured are 0,02 mm and +0,03 mm. Consequently, the tested system has a resolution of 0,10mm and an accuracy of  $\pm 0,03$ mm.
- The test measurements were affected by noise in the linear potentiometer's input and output. The noise in input was created by the 5V line of Arduino DUE and by current flow in the wiper again from the microcontroller. The noise in output was a consequence of these two. Linear potentiometers are purely analog devices, and the output signal is free-of-noise only if the voltage applied is free-of-noise.

- The 12-bit ADC of Arduino DUE suffered from different problems: the 3.3V internal reference is very noisy for high-precision applications and its own nonlinear effects can easily bring back the resolution to 10 bits.
- The analog and the digital circuits have to be separated for high-precision applications: digital devices are very noisy compared to analog equipment.
- An external 12-bit, or even 14-bit or 16-bit, ADC with a separate circuit is needed to have a reliable digital conversion.
- An external low-noise linear stable voltage supply of 5V is necessary for all the components (i.e. microcontroller, external ADC and linear potentiometer) with a reference voltage of 4,096V.
- Voltage followers have to be deployed between the voltage reference and both the linear potentiometer and the external ADC to avoid current flow.
- Finally, it can be disadvantageous to save money on electronics while using high-precision equipment and high-reliability on data is needed.

### 6.3 General observations

The increasing concern about the protection of the architectural heritage has led to a growing interest in SHM as a fundamental tool to improve the structure understanding, reduce uncertainties and provide accurate data for analysis and intervention. On the one hand, it is composed of expensive hardware and complex post-processing software that are limiting its application only on very valuable buildings or highly strategic structures. In this context, the importance of low-cost solution is emerging. On the other hand, many experiences from the software's field have shown the vast possibilities of open-source (O-S) community in terms of efficiency and profitability. In the last few years, a similar trend is moving into hardware. From this background the question: is it possible to build an O-S system that can compete on accuracy and reliability with proprietary systems?

Based on the successful model of O-S software, the purpose of this thesis is to give an initial contribution to the development of an O-S technology for the structural monitoring of historical buildings. The ultimate goal is to start a community that brings together researchers, experts and

enthusiasts creating the resources to continuously improve, debug, solve problems and give advice on O-S SHM. This path could easily generate a reliable, low-cost, efficient and easy to tailor-made technology. Consequently, the large-scale spread of monitoring systems will lead to remarkable growth in the digitalisation of the structural behaviour of historical constructions. A similar project is running by a research team from CERN for the creation of the largest O-S cosmic ray telescope (Cosmic Pi blog<sup>36</sup>) spreading small Raspberry Pi-based platforms all over the world. In addition, the broad availability of O-S digitalised data from structural monitoring can lead to a higher understanding of the architectural heritage's situation, giving to administrators a highly valuable tool to address investments and conservation strategies. Furthermore, the spread of real-time visualisation data can increase the social awareness of the importance of our heritage, fostering other new exploitations (Basto et al., 2017).

As final remark, prototyping with these tools has provided a lot of information to potential user of these systems that are not within the electronics field of knowledge. Research can be afforded and multiplied nowadays (Pearce, 2013). It is important to point out how vital a scientific method is for being robust, reliable and valid.

## 6.4 Suggestion for future improvements

As already stated, a comparable resolution and accuracy with professional solutions are still not accomplished. The future improvements are mainly oriented to solve this issue and to improve system management in a long-run.

- Test the system with uninterruptible power supply (UPS) to avoid sudden switch off.
- In order to drastically cut the expenses, a low-cost solution for the displacement transducer is needed. Some possible improvements are:
  - o Selection of another available market solution beyond the traditional LVDTs and potentiometers, focusing mainly on the price/performance ratio;

---

<sup>36</sup> <http://cosmicpi.org/>

- Developing a high-precision, O-S solution within a multidisciplinary team of mechatronic engineers, electrical engineers and civil engineers that can be directly printed or easily manufactured;
  - Developing a Do It Yourself solution, with a lower-resolution but less complexity.
- Create a printed circuit board (PCB) for the DAS based on the outcomes of paragraph 4.4 to overcome the main limitations related to noisy signal and ADC resolution.
- The remote control can be the solution for the memory problems of Arduino. Through Raspberry Pi, it could be possible to restart the system or modify the sketch directly from the office.
- Deploy the system during laboratory experiments to evaluate its effectiveness in a controlled environment, validating the low-cost system with the professional counterpart.
- Understand the real applicability of low-cost dynamic monitoring of CH buildings.
- Deploy the low-cost system on many different case studies to better understand mid- long-term limitations.



## 7 BIBLIOGRAPHY

- Ali, A. S.; Zanzinger, Z.; Debose, D.; Stephens, B. Open Source Building Science Sensors (OSBSS): A Low-Cost Arduino-Based Platform for Long-Term Indoor Environmental Data Collection. *Build. Environ.* **2016**, *100*, 114–126.
- Allan, A. The State of Boards: Small, Simple Hardware Rules <http://makezine.com/2017/06/27/state-boards-platforms-products-purposes-current-crop-microcontrollers-vies-attention/>.
- Banzi, M. *Getting Started with Arduino (Make: Projects)*; 2008; Vol. 11.
- Basto, C. Study on Possibilities for Low-Cost Monitoring of Historical Structures. Master Thesis, Universitat Politècnica de Catalunya, 2015.
- Basto, C.; Pelà, L.; Chacón, R. Open-Source Digital Technologies for Low-Cost Monitoring of Historical Constructions. *J. Cult. Herit.* **2017**, *25*, 31–40.
- Binda, L.; Saisi, A. The Collapse and Reconstruction of the Noto Cathedral: Importance of the Investigation for the Design Choice TT - Bauinstandsetzen Und Baudenkmalpflege: Eine Internationale Zeitschrift. *Restor. Build. Monum. an Int. J. = Bauinstandsetz. und Baudenkmalpfl. eine Int. Zeitschrift* **2003**, *9* (4), 415–434.
- Binda, L.; Saisi, A.; Tiraboschi, C. Investigation Procedures for the Diagnosis of Historic Masonries. *Constr. Build. Mater.* **2000**, *14* (4), 199–233.
- Binda, L.; Anzani, A.; Saisi, A. Failures due to Long-Term Behaviour of Heavy Structures: The Pavia Civic Tower and the Noto Cathedral. In *Structural studies, repairs, and maintenance of heritage architecture VIII*; 2003; pp 99–108.
- Bisby, L.; ISIS Education Committee. *An Introduction to Structural Health Monitoring*; 2005.
- Bonaccorsi, A.; Rossi, C. Why Open Source Software Can Succeed. *Res. Policy* **2003**, *32* (7), 1243–1258.
- Bretthauer, D. Open Source Software : A History. *UConn Libr. Publ. Work.* **2001**, 1–23.
- Carbonell, J. S. Santa María de Las Arenas, Santa María Del Mar Y El Anfiteatro Romano de Barcelona. *Rev. d'Arqueologia Ponent* **2011**, *21*, 61–73.
- CERN Bulletin. Open Hardware for Open Science. *Cern Bull.* **2011**, 28–29, 5.
- Chacón, R.; Oller, S. Designing Experiments Using Digital Fabrication in Structural Dynamics. *J. Prof. Issues Eng. Educ. Pract.* **2017**, *143* (3).
- DeSantis, T. Resolution vs Accuracy vs Sensitivity Cutting Through the Confusion <https://www.evaluationengineering.com/resolution-vs-accuracy-vs-sensitivity-cutting-through-the-confusion> (accessed Jul 7, 2017).
- Drdácký, M. Structural and Material Health Monitoring of Historical Objects. In *Sensing Issues in Civil Structural Health Monitoring*; 2005; pp 127–133.
- Dunnicliff, J. *Geotechnical Instrumentation for Monitoring Field Performance*; John Wiley & Sons, 1993.
- Ferdoush, S.; Li, X. Wireless Sensor Network System Design Using Raspberry Pi and Arduino for Environmental Monitoring Applications. *Procedia Comput. Sci.* **2014**, No. May, 376–381.
- Gentile, C.; Saisi, A. Ambient Vibration Testing of Historic Masonry Towers for Structural Identification

and Damage Assessment. *Constr. Build. Mater.* **2007**, 21 (6), 1311–1321.

Gentile, C.; Saisi, A.; Cabboi, A. Dynamic Monitoring of a Masonry Tower. In *8th International Conference on Structural Analysis of Historical Constructions (SAHC 2012)*; 2012.

González, R.; Caballé, F.; Domenge, J.; Vendrell, M.; Giráldez, P.; Roca, P.; González, J. L. Construction Process, Damage and Structural Analysis. Two Case Studies. In *Structural analysis of historic construction: preserving safety and significance: proceedings of the Sixth International Conference on Structural Analysis of Historic Construction, 2-4 July 2008, Bath, United Kingdom*; 2008; pp 643–651.

Grosso, A. Del; Lanata, F.; Inaudi, D.; Posenato, D. Data Management and Damage Identification for Continuous Static Monitoring of Structures. *4th World Conf. Struct. Control Monit.* **2004**, 1–8.

Joint Committee for Guides in Metrology. International Vocabulary of Metrology - Basic and General Concepts and Associated Terms (VIM). *JCGM 2002/2012* **2012**, 108.

Kogut, B.; Metiu, A. Open-Source Software Development and Distributed Innovation. *Oxford Rev. Econ. Policy* **2001**, 17 (2), 248–264.

Leach, W. M. Fundamentals of Low-Noise Analog Circuit Design. *Proc. IEEE* **1994**, 82 (10), 1515–1538.

Lorenzoni, F. Integrated Methodologies Based on Structural Health Monitoring for the Protection of Cultural Heritage Buildings. PhD Thesis, University of Trento, 2013.

Lorenzoni, F.; Casarin, F.; Caldon, M.; Islami, K.; Modena, C. Uncertainty Quantification in Structural Health Monitoring: Applications on Cultural Heritage Buildings. *Mech. Syst. Signal Process.* **2015**, 66–67, 268–281.

Mancini, R. Op Amps for Everyone. *Texas Instruments Des. Ref.* **2002**, No. August, 279–280.

Martínez Gil, S. Desarrollo de Herramientas de Fabricación Digital Para La Instrumentación de Estructuras Históricas, Caso de Estudio: Basílica de Santa María Del Mar. Master Thesis, Universitat Politècnica de Catalunya, 2017.

Miller, P.; Moore, D. Precision Voltage References. *Analog Appl. J.* **1999**, No. November, 1–4.

Moon, J. Y.; Sproull, L. Essence of Distributed Work: The Case of the Linux Kernel. *First Monday* **2002**, 10, 381–404.

Murcia, J. Seismic Analysis of Santa Maria Del Mar Church in Barcelona. Master Thesis, Universidad Politécnica de Cataluña, 2008.

Park, J.; Mackay, S.; Wright, E. *Practical Data Communications for Instrumentation and Control*; 2003.

Pearce, J. M. Building Research Equipment with Free, Open-Source Hardware. *Science (80-. )*. **2012**, 337 (6100), 1303–1304.

Pearce, J. M. *Open-Source Lab: How to Build Your Own Hardware and Reduce Research Costs*; 2013.

Ramos, L. F.; Marques, L.; Lourenço, P. B.; De Roeck, G.; Campos-Costa, A.; Roque, J. Monitoring Historical Masonry Structures with Operational Modal Analysis: Two Case Studies. *Mech. Syst. Signal Process.* **2010**, 24 (5), 1291–1305.

Rodriguez, N. How Arduino Is Becoming The World's Social Network For Hackers And Makers <https://www.fastcompany.com/3025320/how-arduino-is-becoming-the-worlds-social-network-for-hackers-and-makers>.



Scherz, P. *Practical Electronics for Inventors*; McGraw-Hill, 2000.

T. C. Carusone, D. A. Johns, K. W. M. *Analog Integrated Circuits Design*; 2012.

Want, R.; Schilit, B. N.; Scott, J. Enabling the Internet of Things. *Computer (Long. Beach. Calif.)*. **2015**, 48 (1), 28–35.

Yen, K. S.; Ratnam, M. M. 2-D Crack Growth Measurement Using Circular Grating Moiré Fringes and Pattern Matching. *Struct. Control Heal. Monit.* **2011**, 18 (4), 404–415.